Cellular Signalling 53 (2019) 374–389

Contents lists available at ScienceDirect

Cellular Signalling

journal homepage: www.elsevier.com/locate/cellsig

Distinct phosphorylation sites/clusters in the carboxyl terminus regulate α_{1D}-adrenergic receptor subcellular localization and signaling

Gabriel Carmona-Rosas, David A. Hernández-Espinosa, Rocío Alcántara-Hernández, Marco A. Alfonzo-Méndez[1], J. Adolfo García-Sainz*

Departamento de Biología Celular y Desarrollo, Instituto de Fisiología Celular, Universidad Nacional Autónoma de México, Ap. Postal 70-248, Ciudad de México 04510, Mexico

ARTICLE INFO

Keywords:
α_{1D}-adrenergic receptor phosphorylation
α_{1D}-adrenergic receptor
Receptor phosphorylation
Membrane localization
Phosphorylation clusters

ABSTRACT

The human α_{1D}-adrenergic receptor is a seven transmembrane-domain protein that mediates many of the physiological actions of adrenaline and noradrenaline and participates in the development of hypertension and benign prostatic hyperplasia. We recently reported that different phosphorylation patterns control α_{1D}-adrenergic receptor desensitization. However, to our knowledge, there is no data regarding the role(s) of this receptor's specific phosphorylation residues in its subcellular localization and signaling. In order to address this issue, we mutated the identified phosphorylated residues located on the third intracellular loop and carboxyl tail. In this way, we experimentally confirmed α_{1D}-AR phosphorylation sites and identified, in the carboxyl tail, two groups of residues in close proximity to each other, as well as two individual residues in the proximal (T442) and distal (S543) regions. Our results indicate that phosphorylation of the distal cluster (T507, S515, S516 and S518) favors α_{1D}-AR localization at the plasma membrane, i. e., substitution of these residues for non-phosphorylatable amino acids results in the intracellular localization of the receptors, whereas phospho-mimetic substitution allows plasma membrane localization. Moreover, we found that T442 phosphorylation is necessary for agonist- and phorbol ester-induced receptor colocalization with β-arrestins. Additionally, we observed that substitution of intracellular loop 3 phosphorylation sites for non-phosphorylatable amino acids resulted in sustained ERK1/2 activation; additional mutations in the phosphorylated residues in the carboxyl tail did not alter this pattern. In contrast, mobilization of intracellular calcium and receptor internalization appear to be controlled by the phosphorylation of both third-intracellular-loop and carboxyl terminus-domain residues. In summary, our data indicate that a) both the phosphorylation sites present in the third intracellular loop and in the carboxyl terminus participate in triggering calcium signaling and in turning-off α_{1D}-AR-induced ERK activation; b) phosphorylation of the distal cluster appears to play a role in receptor's plasma membrane localization; and c) T442 appears to play a critical role in receptor phosphorylation and receptor-β-arrestin colocalization.

1. Introduction

G protein-coupled receptors (GPCRs) are the most abundant class of sensors of the external (light, odors, tastants) and the internal (hormone, neurotransmitters, autacoids) mileaux [1]. These receptors participate in essentially all key physiological processes and are involved in the development of many diseases, making them the target of 20–40% of current therapeutic drugs on the market [2,3]. Among the GPCR family are the adrenergic receptors. These receptors have been classified into α_1-, α_2-, and β-adrenergic subfamilies on the basis of their structure and signaling; each subfamily is formed by three members [4]. In turn, the α_1-adrenergic receptors (α_1-ARs) are composed of the α_{1A}-, α_{1B}- and α_{1D}- subtypes; the latter receptor was the subject of the present work.

As are all the members of the GPCR family, α_{1D}-ARs are constituted of seven membrane-spanning domains connected by three extracellular and three intracellular loops, an extracellular amino terminus, and an intracellular carboxyl tail (CTail) [4]. α_{1D}-ARs have some unique features that have made their study very challenging. For example, α_{1D}-ARs have been difficult to detect in many tissues [5] and, when overexpressed, they have a low level of expression at the plasma membrane, being mainly localized in intracellular vesicles [6–9]. Additionally, α_{1D}-

* Corresponding author at: Inst. Fisiología Celular, UNAM, Ap. Postal 70-248, Ciudad de México 04510, Mexico.
E-mail address: agarcia@ifc.unam.mx (J.A. García-Sainz).
[1] Present Address: Laboratory of Molecular Biophysics, National Heart, Lung, and Blood Institute, NIH, Bethesda, MD 20892, USA.

https://doi.org/10.1016/j.cellsig.2018.11.003
Received 20 September 2018; Received in revised form 8 November 2018; Accepted 8 November 2018
Available online 09 November 2018

ARs have constitutive activity with physiological and pathophysiological relevance; in particular this receptor subtype appears to be involved in the regulation of tissue perfusion and the control of blood pressure, and in the pathogenesis of hypertension [10–20]. Deletion of the first α_{1D}-AR 79 amino acids increases its localization at the plasma membrane [7,8,21–24]. Interestingly, cleavage in the amino terminus occurs endogenously in human cell lines, which suggests that this could be a physiological mechanism employed by cells to generate functional α_{1D}-ARs localized at the plasma membrane [25]. Once at the plasma membrane, α_{1D}-ARs appear to have a conserved mechanism of action: agonist binding to the receptor's extracellular region induces transmembrane conformational changes, which trigger intracellular $G_{q/11}$ -receptor interactions. This activates phosphatidylinositol 4, 5 bisphosphate hydrolysis by PLC-β, generating inositol 1, 4, 5-trisphosphate and diacylglycerol. Inositol trisphosphate causes the release of calcium from intracellular stores, while diacylglycerol is able to activate protein kinase C (PKC) and together these mediators intracellularly propagate the signal. Sustained α_{1D}-AR stimulation triggers the binding of G protein-coupled receptor kinases (GRKs) and the phosphorylation of α_{1D}-ARs third intracellular loops and carboxyl tails, which reduces responsiveness through a mechanism known as homologous desensitization [22–24,26,27]. Additionally, PKC activation induces α_{1D}-AR phosphorylation and reduces responsiveness, a process known as heterologous desensitization [22–24,26,27]. During the former processes, the scaffold protein, β-arrestin, seems to associate with the receptor-signaling complex, favoring the action of the endocytic machinery, receptor internalization, and putatively switching from G protein-mediated to β-arrestin-mediated signaling [28–33].

As compared to other members of the α_1- subfamily, α_{1D}-AR regulatory mechanisms remain poorly characterized. It is known that agonists, such as noradrenaline (NA), and pharmacological activation of PKC by phorbol 12-myristate 13-acetate (PMA) induce phosphorylation and desensitization of α_{1D}-ARs [10,22,26,27]. Using mass spectrometry analysis, our group recently reported distinct α_{1D}-AR phosphorylation patterns in response to NA or PMA [22]; the data suggested possible roles of GRK2 and conventional PKC isoforms α and β in phosphorylations associated with α_{1D}-AR homologous and heterologous desensitization. Six phosphorylated residues in the α_{1D}-AR third intracellular loop (IL3) and nine in the CTail were detected consistently and with high probability [22]. This large number of phosphorylation sites and their location in different receptor domains complicate the experimental analysis of their functional relevance. Hence, the aim of the present work was to further explore the role of some of these residues in α_{1D}-AR function. In order to tackle this issue, we generated several receptor mutants and assessed their phosphorylation state, internalization, and β-arrestin binding, as well as activation of ERK 1/2 and calcium signaling. Here we show that residues located in the carboxyl tail play roles in the signaling and subcellular location of this adrenergic receptor. Our data indicate that there are different points of regulation controlled by phosphorylated residues in close proximity in the α_{1D}-AR CTail.

2. Materials and methods

2.1. Reagents

(−)-Noradrenaline (NA), propranolol, BMY 7378, phorbol myristate acetate (PMA), and lysophosphatidic acid (LPA) were obtained from Sigma-Aldrich Chemical. AG1478 was obtained from Calbiochem and EGF was obtained from Preprotech. [^{32}P]Pi (8500–9120 Ci/mmol) was obtained from Perkin-Elmer Life Sciences. Dulbecco's modified Eagle's medium, fetal bovine serum, trypsin, Lipofectamine 2000, amphotericin B, streptomycin, penicillin, doxycycline hyclate, hygromycin B, blasticidin, and Fura-2 AM were purchased from Invitrogen-Life Technologies. Wheat germ agglutinin Alexa Fluor-350 conjugate (catalog number W11263), Super Signal West Pico chemiluminescence kits, small interfering RNA (siRNA) for β-arrestin 1 (catalog number AM16708, lot AS027ZUU), β-arrestin 2 (catalog number AM16708, lot AS027ZUT), and scrambled siRNA (catalog number AM4611, lot AS026WKE) were obtained from Thermo Fisher. Polyvinylidene difluoride and nitrocellulose membranes were obtained from BioRad. Polyethyleneimine was obtained from Polyscience. Agarose-coupled protein A was obtained from Merck-Millipore. Monoclonal anti-GFP was from Clontech (catalog number 632381, lot A5033481) and polyclonal anti-GFP was generated in our laboratory [22,23,34]. Anti-phospho-ERK 1/2 (Thre202/Tyr204) (catalog number 9101S, lot: 30) and anti-total ERK (p42/44) (catalog number 4695S, lot: 21) antibodies were obtained from Cell Signaling Technology; β-Arrestin-1/2 (catalog number sc-7491, lot D1615) monoclonal antibody was obtained from Santa Cruz Biotechnology (Sc-74,591). Tetramethyl-rhodamine-conjugated AffiniPure anti-donkey mouse IgG (code 715-025-150) was from Jackson Immunology. were purchased from Thermo Fisher Scientific. Secondary antibodies were obtained from Jackson ImmunoResearch and Zymed (Thermo Fisher Scientific). Antibody dilutions were 1:1000 for primary antibodies and 1:10,000 for secondary antibodies.

2.2. Plasmids

cDNA coding for either amino terminus-truncated or amino- and carboxyl termini-truncated-α_{1D}-AR-EGFP (Enhanced Green Fluorescent Protein) constructs (Δ1–79 and Δ1–79 and Δ440–572, respectively [24]) were subcloned into pEGFP-N1 (Clontech). These constructs were further subcloned into pCDNA5/FRT/TO to generate pΔN-α_{1D}-AR-EGFP and pΔNΔC-α_{1D}-AR-EGFP (Flp-ln T-Rex expression system, Invitrogen), as previously described [22]. The latter constructs were mutagenized to change the detected phosphorylated serines and threonine 328 in IL3 [22] into alanines or valine, respectively (S300/323/331/332/334A,T328 V) i. e., plasmids: pΔN-α_{1D}-AR-MutIL3-EGFP and pΔNΔC-α_{1D}-AR-MutIL3-α_{1D}-AR-EGFP. The pΔN-MutIL3-α_{1D}-AR-EGFP construct was then used as a template to mutagenize and generate the following mutants: 1) T442V, 2) S543A, 3) T477V,S486/492A, 4) T507V,S515/516/518A, 5) T477V, S486/492A,T507V,S515/516/518A, 6) T442/477V,S486/492A,T507V, S515/516/518/543A, 7) T477D,S486/492D, 8) T507D,S515/516/518D and 9) T442/477D,S486/492D,T507D,S515/516/518/543D. All these constructs were performed by Mutagenex, Inc. and proper modification was confirmed through sequencing by the same company.

2.3. Cells and transfection

HEK293 cells do not seem to express α_1-ARs as evidenced by the absence of calcium response to NA (in the presence of propranolol) [35] and specific radioligand binding (unpublished). Parental Flp-In T-Rex HEK293 cells (Invitrogen) were grown in Dulbecco's modified Eagle's medium supplemented with 10% fetal bovine serum, 100 μg/ml streptomycin, 100 U/ml penicillin, and 0.25 μg/ml amphotericin B. To generate inducible receptor-expressing cells, parental Flp-In T-Rex HEK293 cells were transfected with pCDNA5/FRT/TO, containing the cDNA coding for the previously described α_{1D}-AR mutants, and pOG44 using Lipofectamine 2000 following the manufacturer's instructions. Transfected cells were selected with 100 μg/ml hygromycin B and 5 μg/ml blasticidin, as previously described [22,36]. Receptor expression was induced with 1 μg/ml doxycycline hyclate 14–24 h before performing experiments. In all experiments using NA, 1 μM propranolol was also present, to avoid any β-adrenergic action; the addition of propranolol by itself had no impact on any of the parameters studied. In experiments in which the expression of β-arrestin 1/2 was knocked down, both the β-arrestin 1 and 2 siRNA (50 nmol final of each plasmid for each 3 cm-diameter dishes) were combined and transfected using Lipofectamine 2000, following the manufacturer's instructions, and cells were cultured for 48 h prior to being used.

2.4. Receptor phosphorylation

Receptor phosphorylation was performed as previously described [22,24]. In brief, cells, cultured in six well plates, were incubated for 3 h in phosphate-free Dulbecco's Modified Eagle's media supplemented with 50 μCi/ml [^{32}P]Pi. Labeled cells were stimulated with the indicated compounds, washed with ice-cold phosphate-buffered saline (PBS) solution and solubilized for 1 h in the lysis buffer [22,24]. The extracts were centrifuged and supernatants were incubated overnight with protein A-agarose and anti-EGFP antiserum. Samples were subjected to SDS-PAGE, transferred onto nitrocellulose membranes and exposed for 24 h. The amount of phosphorylated receptor was assessed by PhosphorImager analysis. Western blotting for loading controls was performed using monoclonal anti-EGFP antibodies.

2.5. Intracellular calcium determinations

Intracellular calcium concentrations were determined as previously described [22,24]. In brief, cells were serum-starved for 2 h, then loaded with 2.5 μM Fura-2/AM for 1 h at 37 °C. Labeled cells were washed three times to eliminate unincorporated dye. Fluorescence measurements were assessed at 340- and 380-nm excitation wavelengths and at a 510-nm emission wavelength, with a chopper interval set at 0.5 s, using an Aminco-Bowman Series 2 Luminescence Spectrometer. Intracellular calcium levels were calculated as described by Grynkiewicz et al. [37].

2.6. ERK 1/2 phosphorylation

Cells were serum-starved for 2 h before experiments. After stimulation with the indicated compounds, cells were washed with ice-cold PBS and lysed with Laemmli sample buffer [38]. Lysates were centrifuged at 12,000 ×*g* for 5 min, and proteins in supernatants were separated by SDS-PAGE. Proteins were electrotransferred onto polyvinylidene difluoride membranes and immunoblotting was performed. Duplicate samples were run in parallel to determine total-ERK and phospho-ERK 1/2. For data normalization, the maximal response was considered as 100%.

2.7. Intracellular fluorescence, receptor internalization and colocalization with endogenous β-arrestin 1/2

Receptor internalization and colocalization assays with endogenous β-arrestin 1/2 were performed as described [22,39]. In brief, cells were seeded to reach 50% confluence into glass-bottomed Petri dishes and were cultured for 24 h at 37 °C in media containing 1% serum and stimulated with NA or PMA. After stimulation, the cells were washed with PBS, fixed with 4% paraformaldehyde in 0.1 M phosphate buffer for 30 min at room temperature, and then washed three times with PBS. To determine intracellular fluorescence and receptor internalization, the plasma membrane was delineated using the differential interference contrast image, and fluorescence in such an area was excluded; intracellular fluorescence was quantified employing ImageJ software [40–42]. To determine membrane-receptor colocalization additional experiments were performed using Alexa Fluor-350-conjugated wheat germ agglutinin (20 μg/ml) for membrane labeling. To determine the colocalization of the α_{1D}-AR with β-arrestin 1/2, the cells were fixed, as indicated previously, and samples were permeabilized with 0.3% Triton X-100 for 15 min at 4 °C. The samples were then incubated with 3% BSA for 1.5 h at room temperature, in the absence or presence of the anti-β-arrestin 1/2 antibody (1:200) with 3% BSA in 50 mM Tris base-buffered saline (pH 7.4) containing 0.1% Tween 20. After this process, the samples were washed twice, were incubated for 2 h in the same buffer containing a tetramethyl-rhodamine-conjugated secondary antibody (1500) and then washed with PBS with soft agitation. Confocal microscopy images were acquired with an Olympus Fluoview FV10 with an oil-immersion objective (60× at 5.0 zoom), 2.0 confocal aperture X16 quality high, and 512 × 512 size. To determine α_{1D}-AR/β-arrestin 1/2 colocalization, the overlap of the two fluorophores (EGFP/rhodamine) was estimated employing ImageJ software [40–42]. Representative images showing green channel fluorescence, red channel

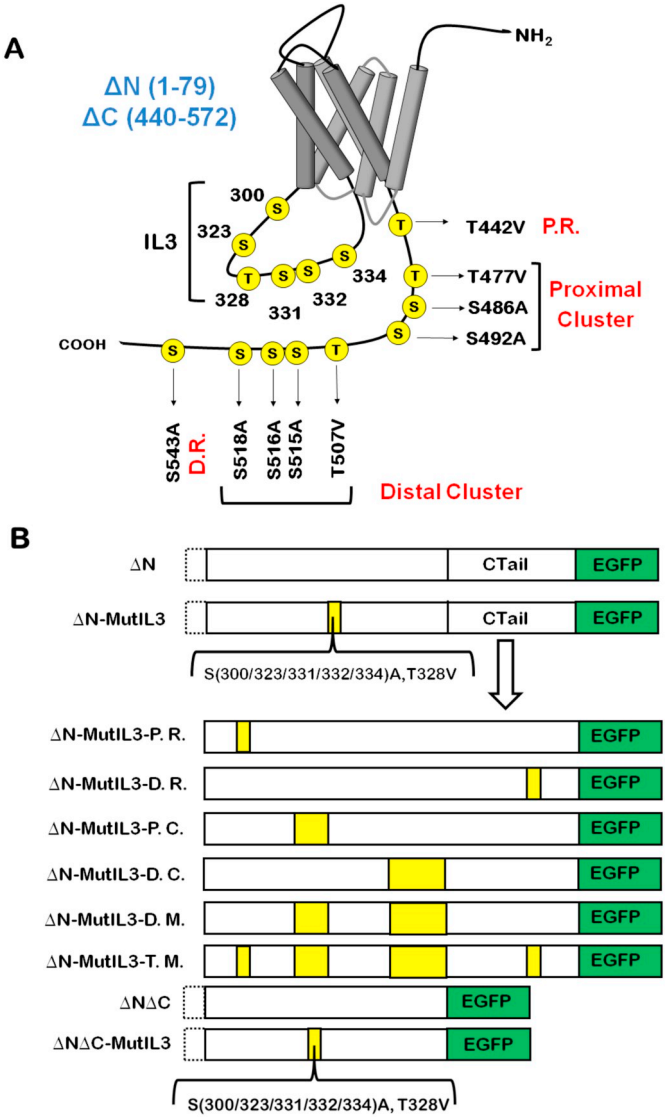

Fig. 1. Schematic representation of the α_{1D}-AR mutants. Panel A: The phosphorylation residues of the α_{1D}-AR detected by MS analysis are located in the IL3 and in the C-terminal tail. Such residues were mutagenized to non-phosphorylatable amino acids: serine residues changed into alanine and threonine residues changed into valine. Panel B: Schematic representation of the α_{1D}-AR mutants. Dotted lines in the constructs represent the deletion of the first 79 amino acids of the N-terminal region (ΔN, 1–79). The mutant ΔN-MutIL3 was generated taking the ΔN receptor as a template. Yellow section in this mutant indicates that the residues S300, S323, S331, S332, S334 and T328 located in the IL3, were mutagenized by non-phosphorylatable residues, as previously described. Subsequently, the ΔN-MutIL3 mutant was mutagenized in T442 (ΔN-MutIL3-P.R.), S543 (ΔN-MutIL3-D.R.), T477, S486, S492 (ΔN-MutIL3-P.C., proximal cluster), T507, S515, S516, and S518 (ΔN-MutIL3-D.C., distal cluster), T477, S486, S492, T507, S515, S516, and S518 (ΔN-MutIL3-D.M.) and T442, T477, S486, S492, T507, S515, S516, S518, and S543 (ΔN-MutIL3-T.M.). Deletion of the last amino acids (440–572) in the CTail (ΔN).

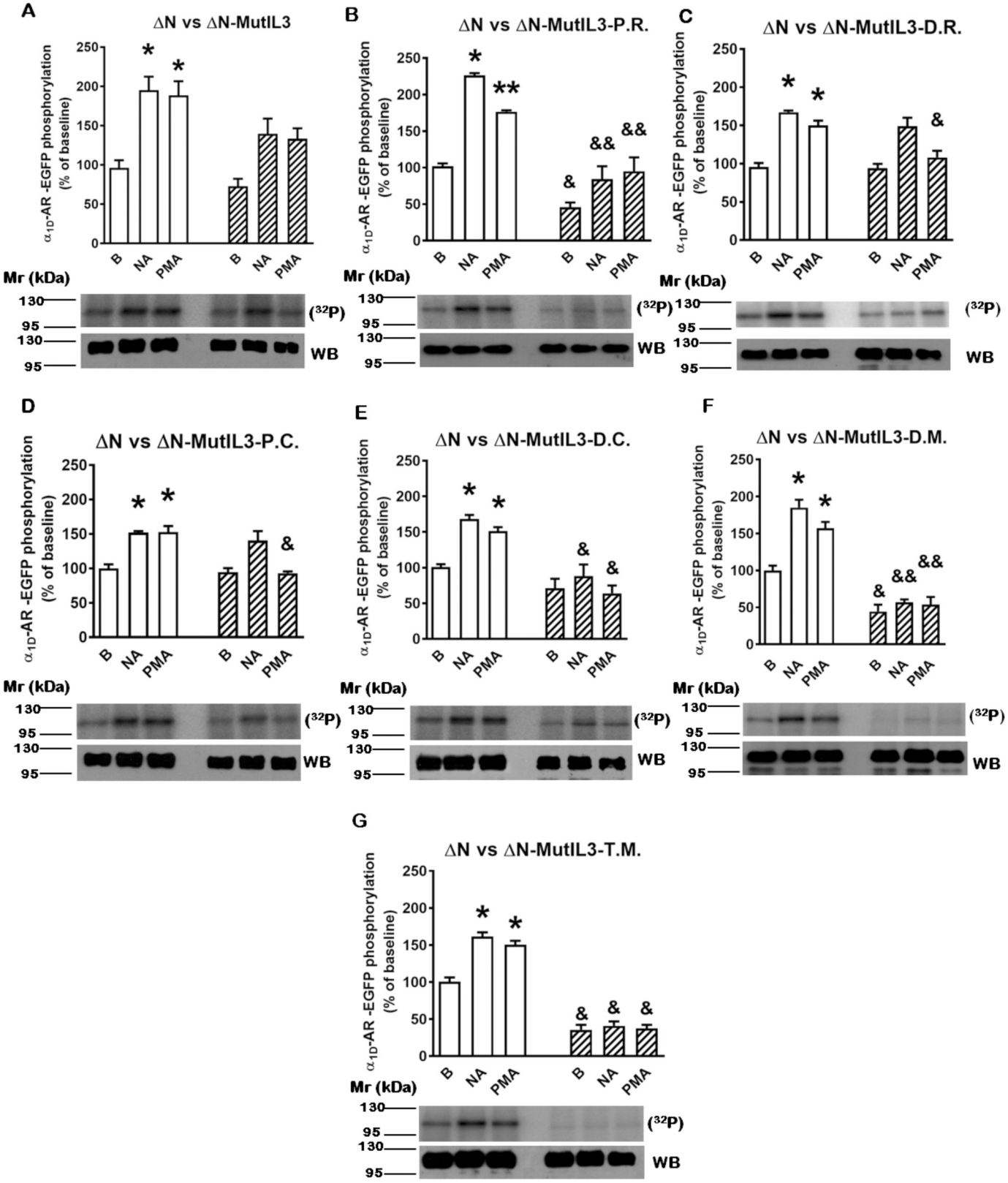

Fig. 2. NA-and PMA-induced phosphorylation of the different α_{1D}-AR mutants. Cells expressing the different constructs were stimulated with NA 10 μM and PMA 1 μM for 15 min and compared to the ΔN receptor. In all cases, cultures were processed in parallel and data were normalized to the percentage of the ΔN receptor's baseline (B) phosphorylation. Plotted lines are the means and vertical lines representing S.E.M. of 3–5 independent experiments. Representative autoradiographs and Western-blots are presented below each graph. Panel 2A, * $P < 0.005$ vs. ΔN receptor's baseline; Panel 2B, *$P < 0.001$ vs, ΔN receptor's baseline, ** $P < 0.005$ vs. ΔN receptor's baseline, & $P < 0.05$ vs. ΔN receptor's baseline, && $P < 0.001$ vs. ΔN receptor's corresponding stimulus; Panel 2C, * $P < 0.001$ vs. ΔN receptor's baseline, & $P < 0.01$ vs. ΔN receptor's PMA; Panel 2D, * $P < 0.005$ vs. ΔN receptor's baseline, & $P < 0.005$ vs. ΔN receptor's PMA; Panel 2E, * $P < 0.005$ vs. ΔN receptor's baseline, & $P < 0.001$ vs. ΔN receptor's corresponding stimulus; Panel 2F, * $P < .005$ vs. ΔN receptor's baseline, & $P < 0.005$ vs. ΔN receptor's baseline, && $P < 0.001$ vs. ΔN receptor's corresponding stimulus; Panel 2G, * $P < 0.001$ vs. ΔN receptor's baseline, & $P < 0.001$ vs. ΔN receptor's corresponding condition.

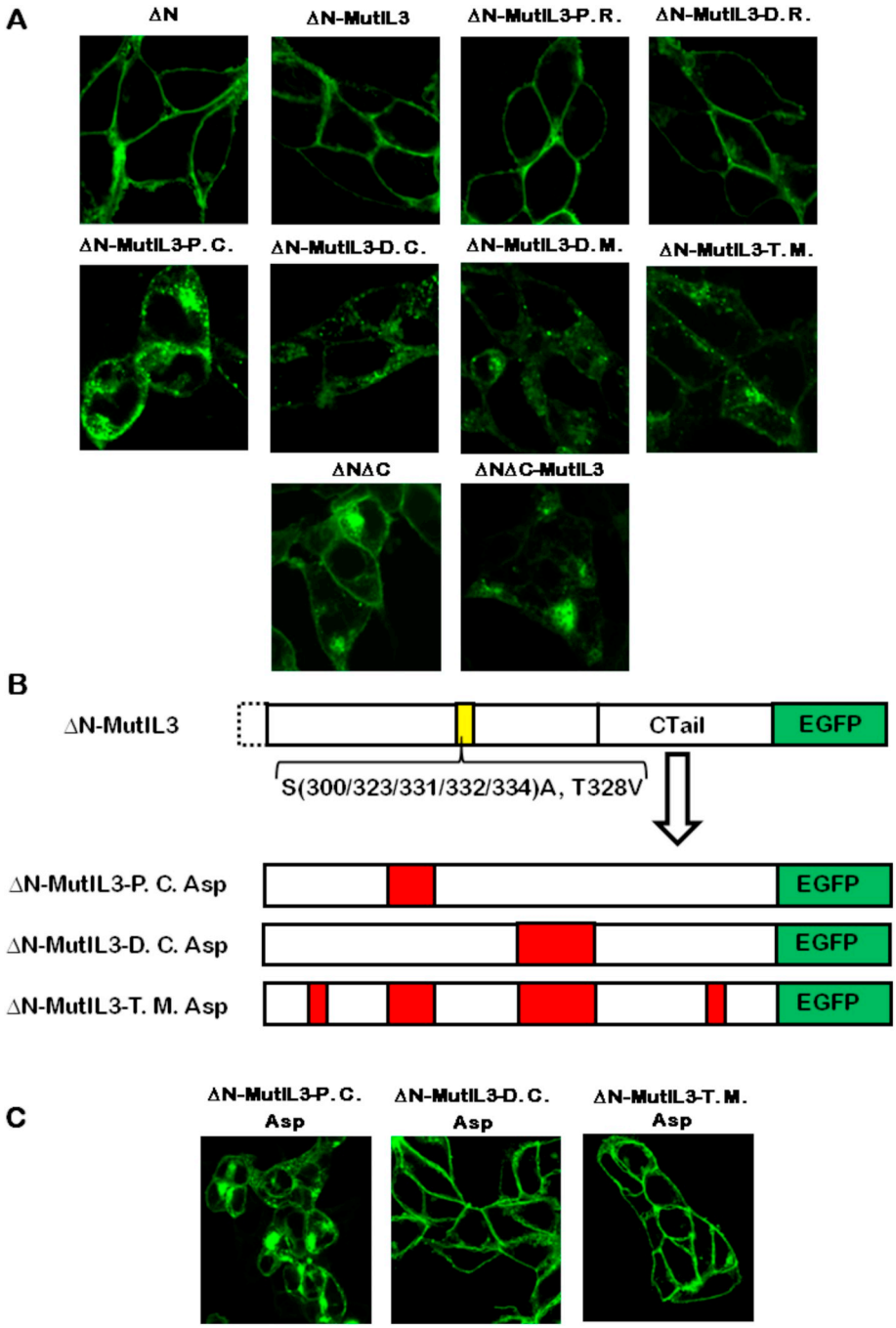

Fig. 3. Subcellular localization of α_{1D}-AR mutants under baseline conditions and schematic representation of the mutants with aspartic acid. Panel A: Cells expressing the different constructs of α_{1D}-AR were analyzed under baseline conditions by confocal microscopy. Images are representative of data of 5–7 experiments using different cell preparations. Panel B: ΔN-MutIL3 was used as a template to change the residues located in the proximal (ΔN-MutIL3-P.C. Asp), and distal cluster (ΔN-MutIL3-D.C. Asp) as well as in both clusters and both proximal and distal residues (ΔN-MutIL3-T.M. Asp), by aspartic acid (phospho-mimetic). Red sections in the constructs represent these mutations. Panel C: ΔN-MutIL3-P.C. Asp, ΔN-MutIL3-D.C. Asp, and ΔN-MutIL3-T.M. Asp mutants were analyzed under baseline conditions by confocal microscopy. Images are representative of data of 5–7 experiments using different cell preparations.

fluorescence, merged images, and pixel-by-pixel colocalization are presented. At least 10 different images per condition were obtained for each experiment.

2.8. Statistical analyses

Statistical comparisons between two conditions was performed employing the Student's *t*-test (Figures 7 and 20; indicated in the text). All other statistical analysis (comparisons between groups with three or more variables) were evaluated using a parametric analysis of variance (ANOVA) with Bonferroni's post-test, assuming Gaussian data distribution (http://www.graphpad.com/guides/prism/7/statistics/index.htm). We utilized the software included in GraphPad Prism 6 software to perform these analyses. A P value < 0.05 was considered statistically significant.

3. Results

3.1. α_{1D}-AR phosphorylation sites and site-directed mutagenesis

Using mass spectrometry, we previously reported that α_{1D}-AR harbors six phosphorylated residues (S300, S323, T328, S331, S332, and S334) in IL3 and nine more on the CTail (see below) [22]. One of the main goals of the present work was to experimentally define the role(s) of the CTail phosphorylation residues. To accomplish this, first we identified that phosphorylation sites in the CTail have a particular arrangement, i.e., two isolated residues (T442 and S543) and two groups of residues with close proximity; we named these groups as proximal cluster (T477, S486, S492) and distal cluster (T507, S515, S516, S518) (Fig. 1A).Taking this arrangement into account, we generated a combination of point mutations and deletions on the α_{1D}-AR (Fig. 1B). As

already mentioned, the α_{1D}-AR amino terminus negatively controls its membrane-targeting [7,8,21–24]. Therefore, all of the mutants were designed using the amino-truncated receptor (ΔN; abbreviated names will be used for clarity). Non-phosphorylatable substitutions in the six residues in IL3 (ΔN-MutIL3) were obtained. These two modifications represent a compromise necessary to obtain: a) membrane expression and b) to eliminate the contribution of phosphorylation at the IL3 in our studies. Then, we used this latter mutant as a template to further individually mutagenize the proximal residue T442 V (ΔN-MutIL3-P.R.) and the distal residue S543A (ΔN-MutIL3-D.R.), as well as the proximal and distal clusters (ΔN-MutIL3-P.C. and ΔN-MutIL3-D.C., respectively). We also included a double mutant where both clusters were changed (ΔN-MutIL3-D.M.) and a total mutant (ΔN-MutIL3-T.M.), including all of these substitutions in the CTail. Finally, we employed the previously reported carboxyl tail-truncated receptor (ΔNΔC) [22] and a further mutated form in which IL3 phosphorylated residues were changed into non-phosphorylatable amino acids (ΔNΔC-MutIL3) [22]. All of these mutants were tagged with EGFP for confocal microscopy imaging and biochemical studies.

Next we utilized Flp-In T-Rex HEK293 cells expressing the former mutants to asses receptor phosphorylation during homologous and heterologous desensitization, i.e., in the presence of 10 μM NA or 1 μM PMA for 15 min. Agents, concentrations, and incubation times were selected based on previously reported data [22]. In independent parallel experiments, the phosphorylation of the ΔN receptor was compared with each of the other mutants and all data were normalized to the phosphorylation of the ΔN receptor detected under baseline conditions. ΔN receptor baseline phosphorylation increased approximately 2-fold after stimulation with NA and PMA, as illustrated in Fig. 2A. In cells expressing the ΔN-MutIL3 receptor, baseline phosphorylation and the actions of NA and PMA were marginally decreased when compared to those of the ΔN receptor (not statistically significant). The CTail mutation on the proximal residue (ΔN-MutIL3-P.R.), resulted in a receptor with decreased baseline labeling and phosphorylation in response to NA and PMA (Fig. 2B). On the other hand, the mutant receptor with the non-phosphorylatable distal residue (ΔN-MutIL3-D.R.) did not exhibit any clear difference in baseline or NA-induced phosphorylation when compared with the ΔN mutant, but the effect of PMA was reduced (Fig. 2C). Similarly, the proximal cluster mutant (ΔN-MutIL3-P.C.) increased its phosphorylation in response to NA, but not after PMA stimulation (Fig. 2D). Interestingly, the receptor with the mutated distal cluster, ΔN-MutIL3-D.C., showed a slight decrease in basal phosphorylation but marked attenuation of phosphorylation observed in response to NA or PMA (Fig. 2E). Baseline phosphorylation of the receptor containing the double-cluster mutations (ΔN-MutIL3-D.M.) diminished below ΔN baseline levels and nearly no effect of NA or PMA was detected (Fig. 2F). Very similar results were obtained with the total mutant (ΔN-MutIL3-T.M.) (Fig. 2G). Overall, these data experimentally confirmed that α_{1D}-AR phosphorylation specifically occurs at the residues depicted in Fig. 1A. It appears that phosphorylatable residues in proximal and distal clusters and distal residue, S543, might be phosphorylated during PMA-induced desensitization and that mutations in the distal cluster also disturb NA-induced phosphorylation. Phosphorylation of ΔNΔC and ΔN-MutIL3-ΔC mutants was reported previously [22].

3.2. α_{1D}-AR plasma membrane localization is regulated by CTail distal cluster phosphorylation

Cells expressing the α_{1D}-AR mutants described previously were studied using confocal microscopy. Under baseline conditions, we observed that the control receptor (ΔN) and the mutant containing substitutions in the IL3 (ΔN-MutIL3), as well as receptors additionally containing single mutations in the proximal and distal residues (ΔN-MutIL3-P.R. and ΔN-MutIL3-D.R., respectively) were mainly located at the plasma membrane. In contrast, receptors including non-phosphorylatable substitutions in the CTail proximal or distal clusters were found mainly in vesicles (Fig. 3A). Prompted by this observation, we measured intracellular fluorescence to qualitatively determine the main subcellular location of each mutant. As depicted in Fig. 4, we normalized all data to the signal detected in the control receptor (ΔN), i. e., it was considered as 100%. As Fig. 4 illustrates, we detected some intracellular fluorescence in ΔN, ΔN-MutIL3, ΔN-MutIL3-P.R. and in ΔN-MutIL3-D.R., whereas the following mutants showed approximately a 4-fold increment of fluorescence located intracellularly: ΔN-MutIL3-P.C., ΔN-MutIL3-D.C., ΔN-MutIL3-D.M. and ΔN-MutIL3-T.M. Moreover, the carboxyl truncated mutants (ΔNΔC and ΔNΔC-MutIL3) revealed a 6-fold increase of intracellular fluorescence. In other words, truncation of the entire CTail or substitutions in the phosphorylation clusters contained in this domain blocked the receptor's ability to reach or remain at the plasma membrane.

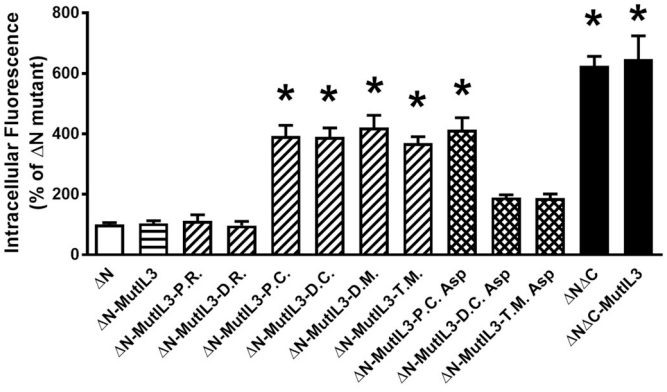

Fig. 4. Intracellular fluorescence quantification (α_{1D}-AR mutants) under baseline conditions. Accumulation of intracellular fluorescence under baseline conditions was quantified for α_{1D}-AR mutants. Data were normalized to that observed in cells expressing the ΔN mutant (100%). Plotted lines are the means and vertical lines representing S.E.M. of 7 independent experiments in each of which 3–5 cells were analyzed (n = 20–35). * $P < 0.001$ vs ΔN.

Under the latter premise, we hypothesized that phosphorylation of such residues in close proximity might regulate receptor subcellular localization. In order to test this, we generated phospho-mimetic mutants containing aspartic acid substitutions. As presented in Fig. 3B, the phosphorylatable residues were changed to aspartic acid in the proximal (ΔN-MutIL3-P.C. Asp) and distal clusters (ΔN-MutIL3-D.C. Asp), as well as in both clusters plus the isolated residues, to generate a total phospho-mimetic mutant (ΔN-MutIL3-T.M. Asp). We observed abundant vesicles in cells expressing ΔN-MutIL3-P.C. Asp (Fig. 3C). This mutant also showed a 4-fold increment of intracellular fluorescence, similar to the mutants lacking phosphorylation clusters (Fig. 4). Surprisingly, ΔN-MutIL3-D.C. Asp and ΔN-MutIL3-T.M. Asp mutants were fully expressed at the plasma membrane (Fig. 3C) and they both showed intracellular fluorescence levels equivalent to the control (intracellular fluorescence quantifications are presented in Fig. 4). In order to confirm these results, colocalization experiments employing Alexa Fluor-350-conjugated wheat germ agglutinin were performed with six of the mutants employed (ΔN, ΔN-MutIL3, ΔN-MutIL3-D.C., ΔN-MutIL3-T.M., ΔN-MutIL3-D.C. Asp and ΔN-MutIL3-T.M. Asp). Wheat germ agglutinin is generally considered as a membrane marker but also binds to glycoproteins present in other organelles [43]. Observations were normalized to the colocalization observed with cells expressing the ΔN mutant. As shown in Fig. 5, in non-permeabilized cells, the lectin labeled the plasma membrane but also some structures present inside the cells; this was much more clearly observed in cells containing large amounts of vesicles. Despite this, the colocalization data (Fig. 5) confirmed the previous findings (Fig. 4). Altogether, these results suggest that, specifically, distal-cluster phosphorylation could be necessary and sufficient to allow α_{1D}-AR plasma membrane localization.

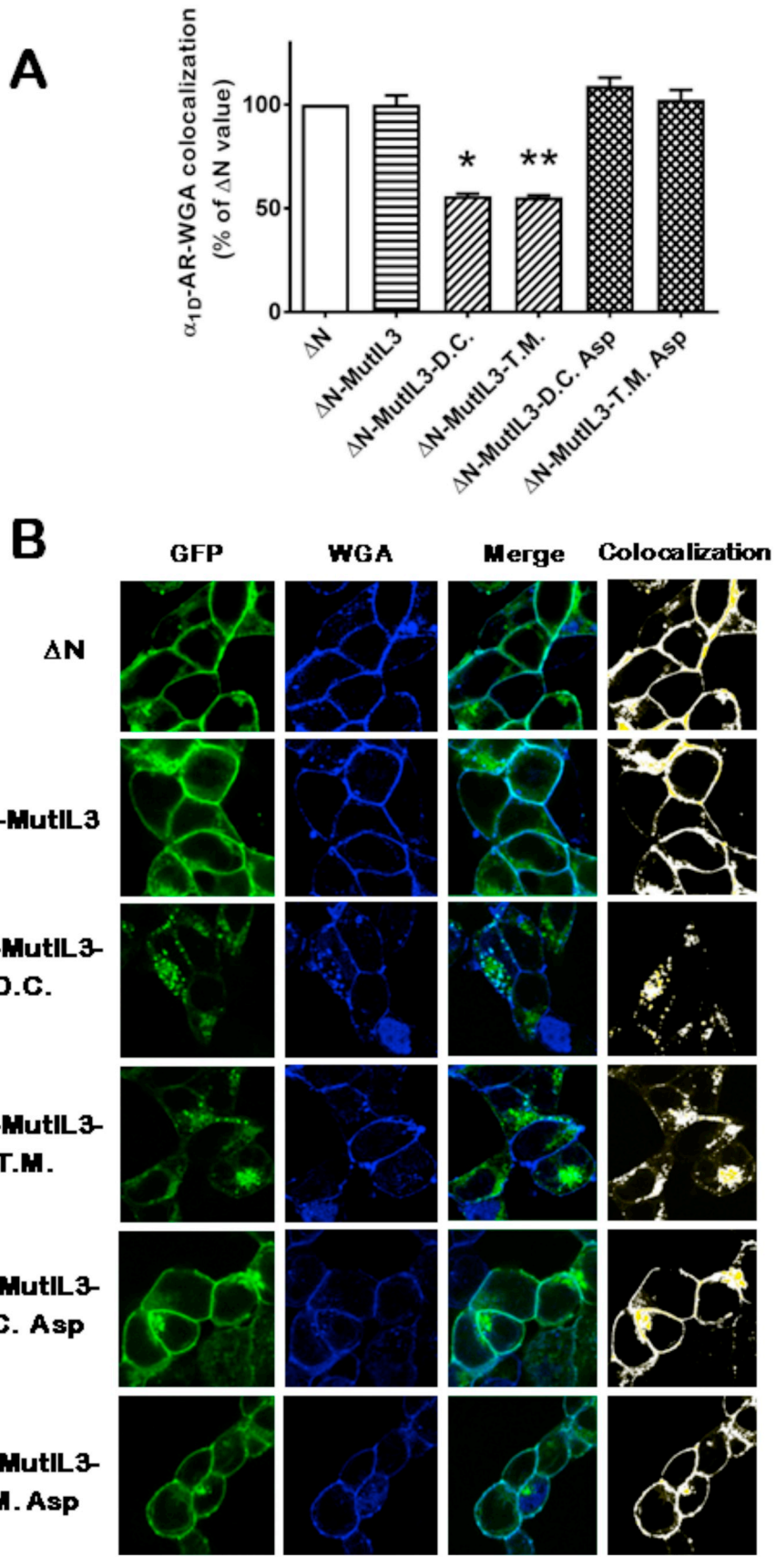

Fig. 5. Colocalization of α_{1D}-AR mutants with Alexa Fluor-350-conjugated wheat germ agglutinin (plasma membrane marker) under baseline conditions. Cells expressing the different constructs of α_{1D}-AR were fixed and stained with Alexa Fluor-350-conjugated wheat germ agglutinin (WGA), as indicated under Material and Methods. Fluorescence was analyzed under baseline conditions by confocal microscopy and ImageJ analysis. Panel A, Receptor-membrane marker colocalization, normalized to ΔN mutant baseline value (100%), is presented. Plotted are the means and vertical lines representing S.E.M. of 4 independent experiments in each of which 10 cells were analyzed ($n = 40$). * $P < 0.001$ vs. ΔN mutant and $P < 0.001$ vs. ΔN-MutIL3-D.C. Asp; ** $P < 0.001$ vs. ΔN mutant and $P < 0.001$ vs. ΔN-MutIL3-T.M. Asp. Panel B, representative images showing: receptor fluorescence (GFP), WGA fluorescence, Merge images and colocalization (white).

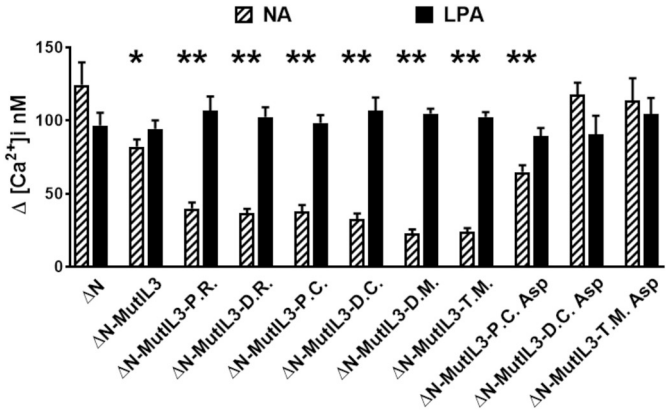

Fig. 6. NA- and LPA-induced mobilization of intracellular calcium in cells expressing the different α_{1D}-AR mutants. Cells expressing the different constructs were stimulated with NA 10 μM (dashed bars) or LPA 1 μM (solid bars) and increases (Δ $[Ca^{2+}]$ i nM; baseline subtracted) in intracellular calcium concentration were determined. Plotted are the means and vertical lines representing S.E.M. of 5–7 independent experiments. * $P < 0.005$ vs. ΔN, NA-stimulation; * $P < 0.001$ vs. ΔN, NA-stimulation. No significant difference was observed when the response to LPA stimulation in the different cell lines was compared.

3.3. Phosphorylation on α_{1D}-AR CTail specific residues regulates the mobilization of intracellular Ca^{2++}

Next, we evaluated agonist-induced mobilization of intracellular calcium to determine the functionality of the receptors previously described. As depicted in Figs. 6, 10 μM NA elicited an increase of over 100 nM intracellular calcium in cells expressing the ΔN receptor, whereas it scarcely reached 100 nM in cells expressing the ΔN-MutIL3 mutant. Remarkably, in CTail mutants lacking phosphorylatable single residues or clusters (ΔN-MutIL3-P.R., ΔN-MutIL3-D.R., ΔN-MutIL3-P.C., and ΔN-MutIL3-D.C.), calcium release was markedly reduced as compared with those expressing the ΔN receptor. Calcium increments were even smaller in double and total mutants (ΔN-MutIL3-D.M. and ΔN-MutIL3-T.M.). As a positive control, we measured the response of endogenously expressed lysophosphatidic acid receptors, using 1 μM LPA, and a consistent increase in calcium concentration (≈ 100 nM) was observed in cells expressing the different mutants. When we examined receptors containing the phospho-mimetic mutations, we observed that the proximal cluster mutant (ΔN-MutIL3-P.C. Asp) partially recovered its ability to mobilize intracellular calcium. Interestingly, distal cluster and total mutants containing the phospho-mimetic mutations (ΔN-MutIL3-D.C. Asp and ΔN-MutIL3-T.M. Asp) were able to increase calcium to concentrations similar to those of the control (ΔN receptor-expressing cells). These data suggest that phosphorylation of the CTail region, mainly at the distal cluster, controls the ability of α_{1D}-AR to trigger the calcium signaling pathway. NA-induced increases in intracellular calcium in cells expressing the ΔNΔC and ΔN-MutIL3-ΔC mutants were reported previously [22]. The effect of NA on intracellular calcium concentration as affected by NA, PMA and BMY 7378 (inverse agonist) [10,11,24] is presented in Supplementary Fig. S1. In agreement with the previous data, NA action was robust in cells expressing the ΔN mutant; this was of smaller magnitude in cells expressing the ΔN-MutIL3 mutant and even smaller in cells expressing the ΔN-MutIL3-T.M. receptors. Similarly, the ability of PMA and BMY 7378 was very clear in cells expressing the ΔN mutant and marginal (but statistically significant) in cells expressing the total mutant (Supplementary Fig. S1).

3.4. α_{1D}-AR mutants' ERK activation kinetics

A different pathway initiated by α_{1D}-AR was investigated. ERK 1/2 phosphorylation was determined under baseline conditions and after 2, 5, 15, 30, and 60 min of incubation with 10 μM noradrenaline. As it is shown in Fig. 7A, the ΔN mutant showed a rapid increase in ERK phosphorylation after 5 and 15 min, and subsequently, this signal decreased at 30 and 60 min. In the same way, the rest of the mutants also presented a quick increase in ERK 1/2 phosphorylation. However, the signal remained elevated in all of these even after 60 min of observation (this trend was statistically significant (Student's *t*-test $P < 0.05$; 60 min vs. ΔN mutant) except for the ΔN-MutIL3-D.R. and ΔN-MutIL3-D.M. mutants). Representative Western blots of the p-ERK 1/2 and total-ERK 1/2 of each mutant are presented (Fig. 7B).

3.5. α_{1D}-AR activation of ERK is regulated by the transactivation of the EGF receptor and β-arrestins

It has been observed that α_{1D}-AR activation induces the shedding of active epidermal growth factor (EGF) that stimulates the EGF receptor and contributes to the activation of ERK 1/2 [44]. Fig. 8A shows that when cells expressing the ΔN receptor are treated with EGF, a robust increase in ERK 1/2 phosphorylation can be detected. AG1478, a specific inhibitor of EGF receptor endogenous tyrosine kinase activity [45] totally abolished the EGF effect. Cells stimulated with NA for 5 min, also showed an important increase in ERK 1/2 phosphorylation; interestingly, this activation was markedly diminished when the cells were pre-incubated with AG1478 and then challenged with NA (Fig. 8A). It has been shown that activation of ERK depends in some cells on the binding of β-arrestins to GPCRs, forming a multi-protein complex: GPCR/β-arrestin/ERK1/2 [32]. In order to explore the possible participation of β-arrestins, we knocked down the expression of β-arrestin 1/2 by using small interfering RNA. Fig. 8B illustrates the increase in ERK 1/2 phosphorylation when cells expressing the ΔN mutant were stimulated with NA for 5 and 60 min. Scrambled small interfering RNA induced a very small decrease (not statistically significant) of NA-induced ERK phosphorylation, as presented in the same figure. In contrast, when β-arrestin1/2 was knocked down, a clear decrease of NA-induced ERK phosphorylation was detected, at 5 and 60 min. β-arrestin 1/2 knock down was confirmed by Western blot analysis (Fig. 8B). The roles of EGF receptor transactivation and of β-arrestin 1/2 knock down were also tested in cells expressing the ΔN-MutIL3-T. M. mutant and the results were very similar, i. e., data confirmed the role of these processes in α_{1D}-AR ERK 1/2 activation (Supplementary Fig. S2). Overall, these experiments suggest that transactivation of EGF receptors and β-arrestins participate in NA-induced ERK 1/2 activation, in cells expressing the receptor mutants employed.

3.6. The α_{1D}-AR mutants have a different kinetic of internalization triggered by NA and PMA

α_{1D}-AR internalization using confocal microscopy was studied next. In order to achieve this, we exclusively studied the mutants that were mainly expressed at the plasma membrane under baseline conditions. Attempts to study this with mutants that were mainly internalized proved to be impossible with this approach. To evaluate the kinetic profiles of internalization, cells were stimulated with NA or PMA. The intracellular fluoresce of cells expressing each mutant, under baseline conditions, was considered as 100% (Figs. 9 and 10); these baseline values were very similar as shown in Fig. 4. As depicted in Fig. 9A, we stimulated the cells with NA 10 μM and detected an increase in the intracellular florescence at 5 and 15 min in the ΔN mutant. Subsequently, the intracellular signal vanished and was barely detected at 30

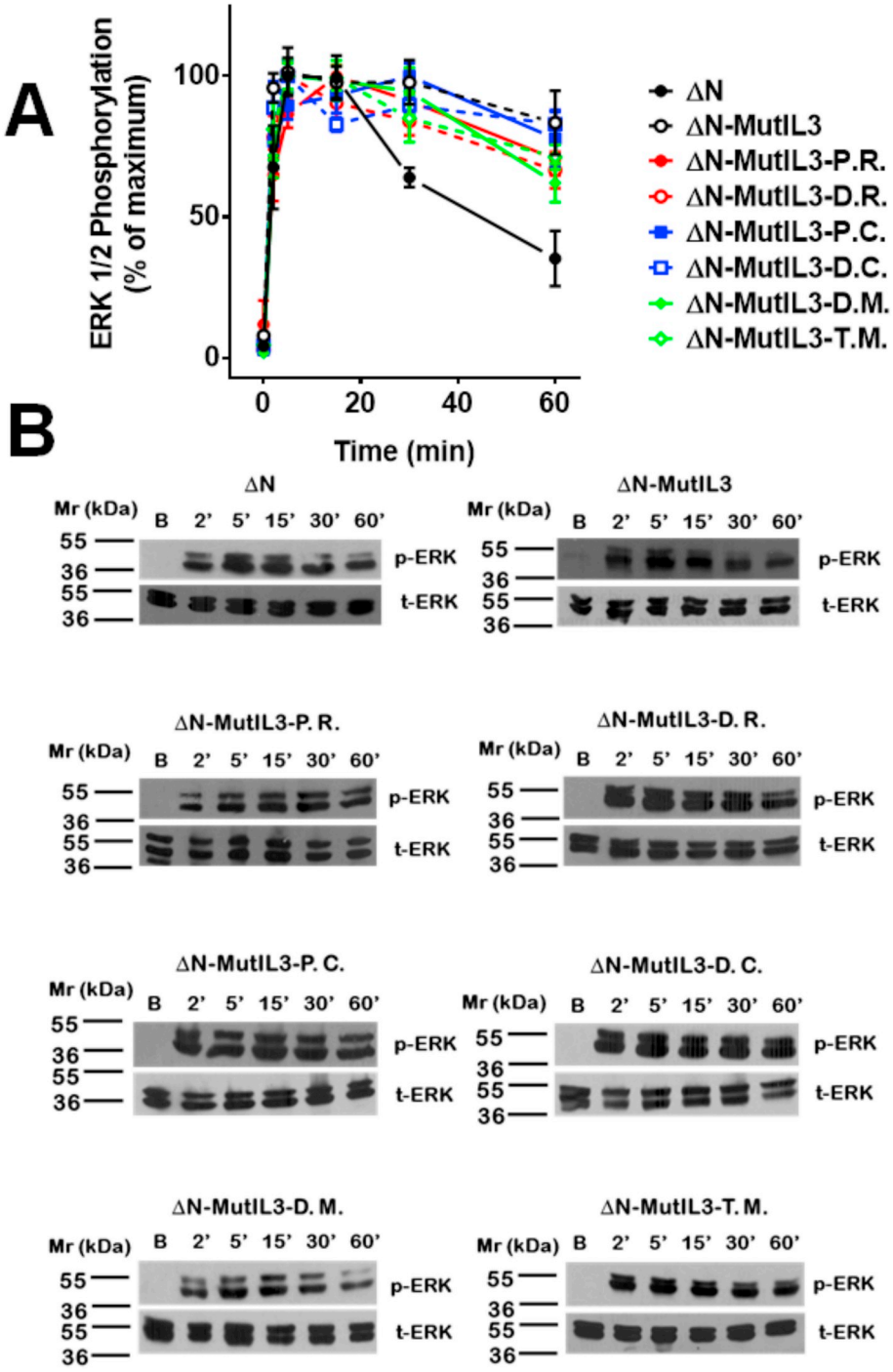

Fig. 7. Time-course of NA-induced activation of ERK1/2 in the different α_{1D}-AR mutants. Cells expressing the different constructs were stimulated for the times indicated with NA 10 μM, and ERK1/2 phosphorylation was determined. Plotted lines are the means and vertical lines representing S.E.M. of at least 4 independent experiments. Representative Western-blots for total-ERK1/2 and phospho-ERK1/2 are presented below the graph.

and 60 min. The ΔN-MutIL3 mutant was also internalized in response to NA, but remained so, along the 60 min of stimulation (Student's *t*-test vs. the ΔN mutant, $P < 0.001$at 60 min). Interestingly, the ΔN-MutIL3-P.R. and ΔN-MutIL3-D.R. mutants behaved in a similar manner to those of the ΔN mutant, i.e., there was an increase in intracellular fluorescence at 5 and 15 min and a partial decrease of such a signal at 30 and 60 min (Student's t-test: $P < 0.001$ vs. the ΔN mutant and $P < 0.001$ vs. the ΔN-MutIL3 mutant at 60 min). Fig. 9B presents the images of the kinetic profiles of internalization of each α_{1D}-AR mutant.

Next, we decided to evaluate the kinetic profile of internalization of the same mutants by stimulating the cells with 1 μM PMA. As shown in Fig. 10A, we detected that the ΔN mutant progressively internalized during the 60 min of incubation. In contrast, the ΔN-MutIL3 reached the maximal internalization at 15 min and then intracellular fluorescence

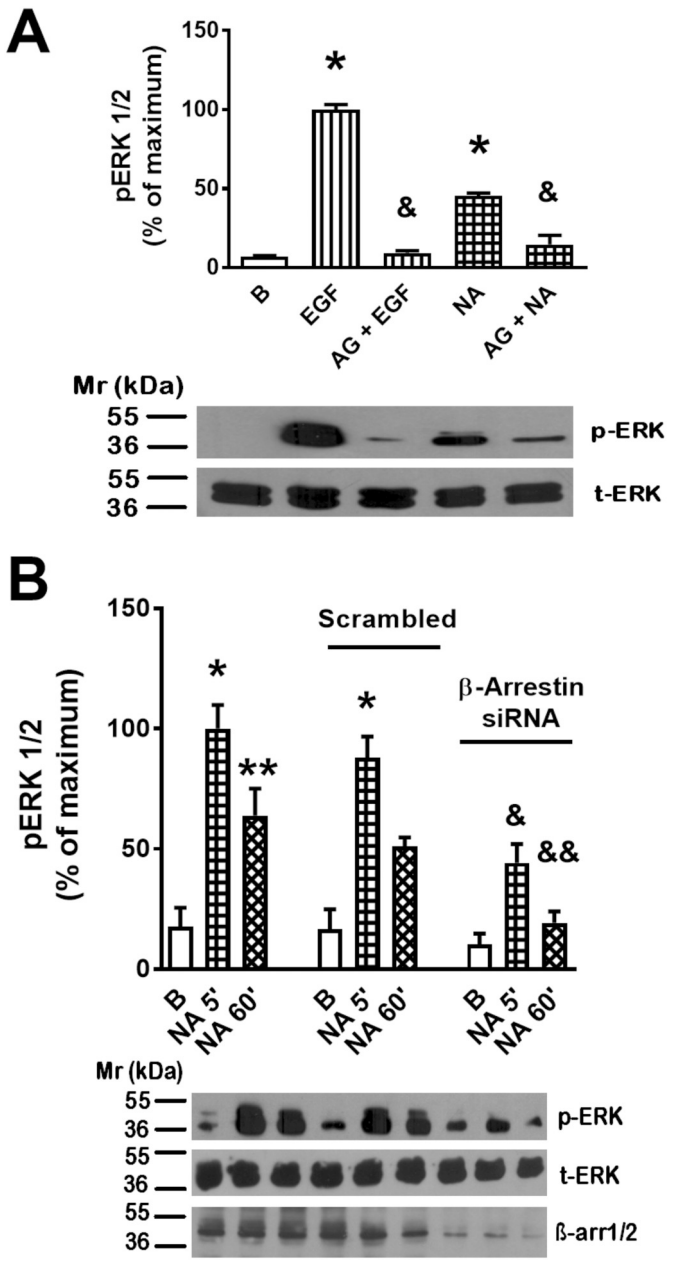

Fig. 8. Regulation of ERK 1/2 phosphorylation by EGF receptor transactivation and β-arrestins in cells expressing the ΔN receptor. Panel A: Cells were pre-incubated in the absence or presence of AG1478 10 μM (AG) and then challenged with EGF 100 ng/ml or NA 10 μM for 5 min. Plotted are the means and vertical lines representing the S.E.M. of 3 independent experiments. * $P < 0.001$ vs. baseline (B); & $P < 0.001$ vs. absence of AG1478. Representative Western-blots for total-ERK 1/2 and phospho-ERK 1/2 are presented below the histogram. Panel B: Cells were nor transfected (first group or bars), or they were transfected with either a scrambled siRNA (second group of bars) or with a specific siRNAs to block the expression of β-arrestin 1/2 (third group of bars) Cells were stimulated with NA 10 μM for 5 (5′) or 60 min (60′). Plotted are the means and vertical lines representing S.E.M. of 3 independent experiments. * $P < 0.001$ vs. respective baseline (B); ** $P < 0.05$ vs. respective baseline (B); & $P < 0.005$ vs NA 5′ non-transfected cells and $P < 0.05$ vs. NA 5′ scrambled siRNA; && $P < 0.05$ vs. NA 60′ non-transfected cells. Representative Western-blots for total-ERK 1/2, phospho-ERK 1/2, and β-arrestins (β-arr1/2) are presented below the histogram.

gradually decreased toward baseline values (Fig. 10A, Student's *t*-test vs. the ΔN mutant, $P < 0.001$ at 60 min). The ΔN-MutIL3-P.R. similarly reached its maximal internalization at 15 min,but intracellular fluorescence remained at that level during the remaining of the incubation (Student's t-test vs. the ΔN mutant and ΔN-MutIL3 mutant, $P < 0.001$ in both comparison, at 60 min). The ΔN-MutIL3-D.R. mutant behaved like the ΔN-MutIL3 mutant (Fig. 10A, Student's t-test vs. the ΔN mutant, $P < 0.001$ at 60 min). Fig. 10B presents representative images of the kinetic profile of internalization of each α_{1D}-AR mutant under the action of PMA.

3.7. The α_{1D}-AR mutants colocalize with endogenous β-arrestin1/2

β-arrestins are scaffold proteins known to bind and participate in the internalization of ligand-activated receptors. This process allows for a GPCR to maintain signaling while internalized in endosomes in a β-arrestin-dependent fashion [29,46,47]. Hence, we examined the colocalization of endogenous β-arrestins with the α_{1D}-AR mutants that are expressed at the plasma membrane, taking into consideration the time at which each mutant was maximally internalized in response to NA or PMA. Data were normalized to the colocalization observed, under baseline conditions, in cells expressing each mutant. As it is shown in Fig. 11A, colocalization was observed under baseline conditions with all of the cells studied and mainly at the plasma membrane (Fig. 11B); this could be due to the α_{1D}-AR intrinsic activity. However, this was less clear with the ΔN-MutIL3-P.R mutant (Fig. 11B). When cells were treated with NA or PMA, the ΔN, ΔN-MutIL3 and ΔN-MutIL3-Δ-D.R. mutants increased their colocalization with endogenous β-arrestin1/2, and colocalization was also clearly observed intracellularly (Fig. 11, panels A and B). Interestingly, the ΔN-MutIL3-ΔP.R. mutant did not increase its colocalization with β-arrestins in response to NA or PMA. Representative images of the colocalization of each mutant with endogenous β-arrestin1/2, under the conditions described, are illustrated in Fig. 11B. When the primary anti-β-arrestin antibody was omitted during the immunostaining procedure, essentially no fluorescence was observed in the red channel and consequently no colocalization was detected; these data indicate that the observed fluorescence was due to detection of the anti-β-arrestin antibody and not to unspecific immunostaining by the secondary antibody (Supplementary Fig. S3). Colocalization of α_{1D}-AR and β-arrestin was absent in cells expressing receptors located in intracellular vesicles (data not shown). It must be stated that colocalization does not necessarily imply physical interaction of these proteins.

4. Discussion

α_{1D}-AR is known for being an elusive GPCR, whose expression, cellular localization, and function, as well as its roles in the development of cardiovascular diseases and other maladies, remain only partially known to date [48–51]. The ability of agonists and phorbol esters to induce α_{1D}-AR phosphorylation and the association of this process with receptor desensitization has been known for some time [22–24,26,27]. A series of α_{1D}-AR phosphorylation sites were recently defined by employing mass spectrometry [22]. This latter work revealed that there are six phosphorylated residues located in the IL3 and nine in the CTail, and that several protein kinases could putatively target such residues, including PKC α/β and GRK2. In our present experiments, we observed that as the phosphorylation sites were substituted by non-phosphorylatable amino acids, baseline phosphorylation, as well as those observed in response to receptor activation (NA) or PKC stimulation (PMA), decreased. Therefore, the identified 15 amino acids seem to be the major targets of the protein kinases involved

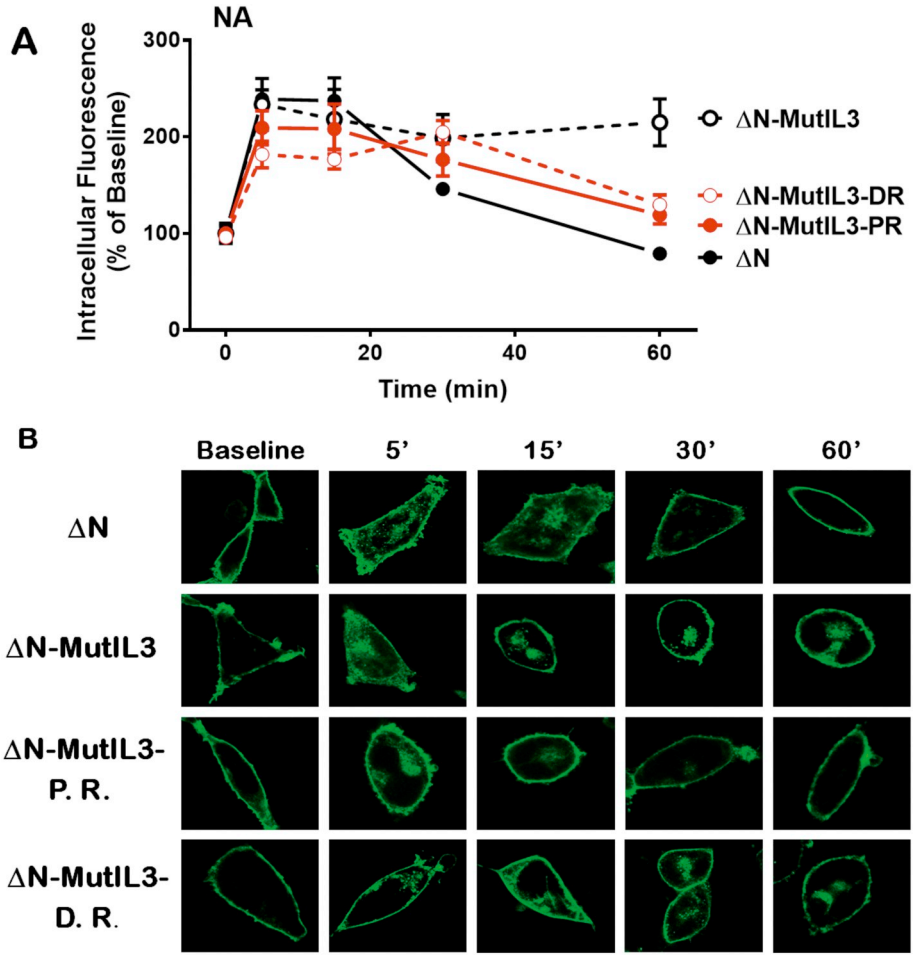

Fig. 9. Time-course of NA-induced internalization of the different α_{1D}-AR mutants. Panel A: Accumulation of intracellular fluorescence in response to NA 10 μM in cells expressing the ΔN, ΔN-MutIL3, ΔN-MutIL3-P.R. and ΔN-MutIL3-D.R. mutants. The intracellular fluorescence observed, under baseline conditions, in cells expressing each of the mutants was considered as 100%. Plotted are the means and vertical lines representing S.E.M. of 7 independent experiments in each of which 3–5 cells were analyzed (n = 20–35). Panel B: Representative images.

in α_{1D}-AR phosphorylation. However, in the total mutant, i. e. in the receptor in which all the 15 detected residues were substituted by non-phosphorylatable amino acids, a very weak but consistent receptor phosphorylation was detected, including some marginal actions of NA and PMA. It is important to consider that the reported phosphorylated residues were those that were consistently detected in the different mass spectrometry analysis performed and with high probability (i. e., high Ascore value [52]) [22]. However, during the course of that study, other phosphorylation sites were detected, although not in all the analysis or with low probability value. Therefore, it is possible that the remaining phosphorylation detected could be due to such sites. It should be mentioned that in our previous experiments using the mutant, ΔNΔC-MutIL3 (in which the amino and carboxyl termini were deleted and the identified phosphorylated sites at the IL3 were substituted by non-phosphorylatable residues), we were unable to detect receptor phosphorylation and no evidence for stimulation by NA or PMA were observed [22]. These data suggest the possibility that the unidentified phosphorylation site(s) could be present at the CTail.

Interestingly, the ΔN-MutIL3-P.R. mutant in which the proximal residue, T442, was modified to valine showed a decrease in baseline as well as in stimulated (NA and PMA) receptor phosphorylation. Such decrease was much larger than could have been anticipated, because only one of the phosphorylation targets was modified. This might suggest that such a residue could be an important regulator of total receptor phosphorylation. In addition, this mutant, although mainly localized at the plasma membrane, appears to colocalize poorly with β-arrestins in response to NA or PMA. This could be related with its decreased phosphorylation, since it has been shown structurally that phosphorylation of CTail peptides is critical for β-arrestin binding [53]. However, we cannot discard the possibility that the amino acid substitution could alter the structure in such a way that both receptor phosphorylation and colocalization with β-arrestins could be perturbed. GPCR association with β-arrestins has been mainly observed during homologous desensitization and the information of such possible interaction during heterologous desensitization is scarce; our present data suggest that this takes place in the course of both processes.

We previously observed that an amino- and carboxyl-termini-truncated receptor (i. e., the ΔNΔC α_{1D}-AR mutant) was able to increase intracellular calcium (G protein signaling) and could be desensitized by PKC activation [18]. The lack of the CTail altered the mitogen activated kinase pathways in some cells (Rat-1 fibroblasts or neuroblastoma B103), but not in the HEK cell line [17]. We also observed that mutants lacking the CTail (i. e., the ΔNΔC and ΔNΔC-MutIL3 receptors) were mainly localized in intracellular vesicles [16], which was confirmed in the present work. It has been reported that the α_{1D}-AR CTail is of importance for this receptor's proper plasma membrane targeting/insertion, because interaction with proteins such as syntrophins seems to be involved and this takes place through the receptor's CTail-located PDZ domain [44,45].

One of the major findings of the present work is the relationship between phosphorylatable residues and α_{1D}-AR cellular localization. As already mentioned, current ideas indicate that GPCR phosphorylation

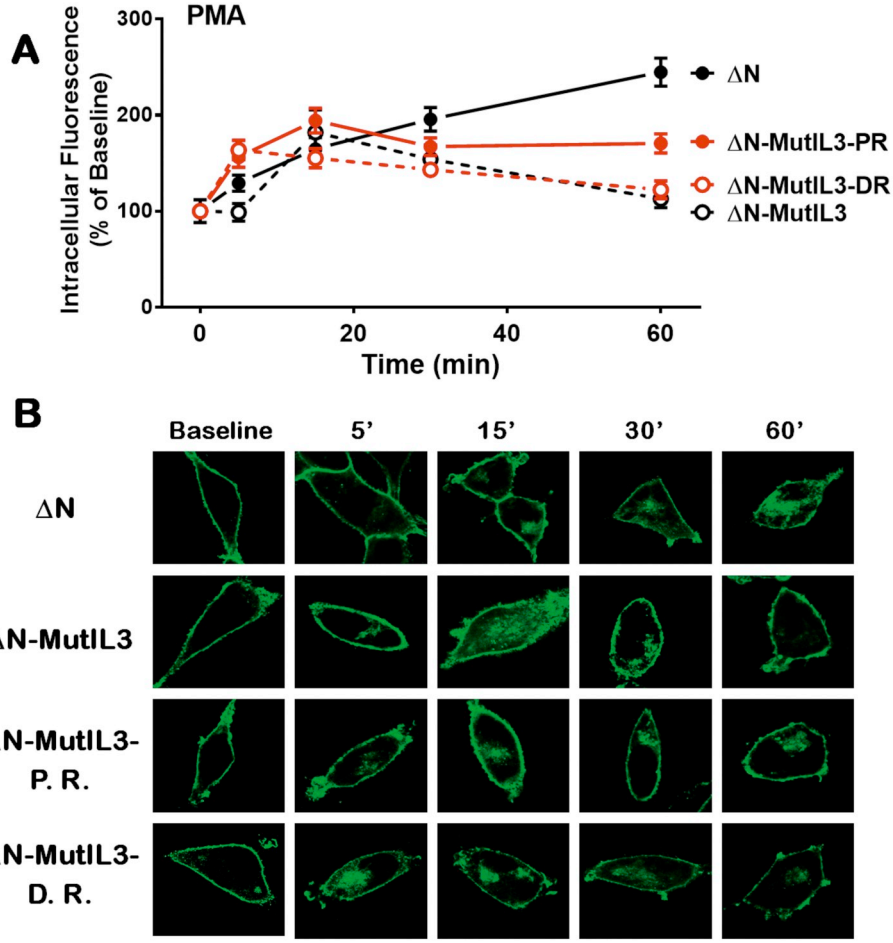

Fig. 10. Time-course of PMA-induced internalization of the different α_{1D}-AR mutants. Panel A: Accumulation of intracellular fluorescence in response to PMA1 μM in cells expressing the ΔN, ΔN-MutIL3, ΔN-MutIL3-P.R. and ΔN-MutIL3-D.R. mutants. The intracellular fluorescence observed, under baseline conditions, in cells expressing each of the mutants was considered as 100%. Plotted are the means and vertical lines representing S.E.M. of 7 independent experiments in each of which 3–5 cells were analyzed (n = 20–35). Panel B: Representative images.

triggers an association with the scaffold protein, β-arrestin, favoring the action of the endocytic machinery, receptor internalization and putatively switching from G protein-mediated signaling to β-arrestin-mediated action [28–33]. Some of the present results indicate that not all GPCR phosphorylations trigger receptor internalization, but rather the opposite: these results were totally unexpected and extremely puzzling, but at the same time, are provocative and their interpretation is challenging.

Our data indicate that the phosphorylation state of residues T507, S515, S516, and S518, which are located in the distal cluster of the C-terminal tail, regulate the subcellular localization of α_{1D}-ARs. When these residues were exchanged for non-phosphorylatable amino acids, the α_{1D}-ARs were localized mainly in intracellular vesicles. This was contrary to our expectations; i. e., we anticipated that the absence of phosphorylation sites would favor receptor retention at the plasma membrane. The possibility that the amino acid substitutions could alter the receptor's conformation was considered, but substitution of these same residues for the phospho-mimetic amino acid, aspartic acid, restored the receptor's plasma membrane localization. This is completely counter to the general idea that all GPCR phosphorylations could be functionally translated into desensitization, internalization, and possible degradation, and that a general action of protein phosphatases might trigger receptor recycling. The present findings suggest that these processes are more complex than anticipated and that it is likely that phosphorylation at some specific sites could lead to internalization, whereas at others this might favor membrane localization. To the best of our knowledge, this is the first study indicating that the phosphorylation of certain residues in a GPCR CTail could favor receptor localization at the plasma membrane. However, it must be mentioned that it has been reported that prolonged inhibition of PKC induces down-regulation of sphingosine 1-phosphate $S1P_1$ receptor surface expression, associated to decreased receptor phosphorylation, but the mechanisms or residues involved were not explored [54]. Similarly, there is evidence that phosphorylation of channel receptor (also called "ionotropic receptors") subunits, such as those of AMPA/Glutamate receptors or $GABA_A$ receptors increase their membrane localization (see, for example [55–58]).

The steady state density of plasma membrane receptors results from a balance between several complex processes, i. e., anterograde transport and insertion into the plasma membrane, internalization and recycling. Intracellular accumulation of receptors might result from decreased plasma membrane insertion, by a reduced time of residence in this organelle due to increased internalization or improper recycling; these events are not mutually exclusive and combinations might exit in response to key structural modification. The absence of α_{1D}-AR phosphorylation sites, in the distal CTail cluster, could render membrane targeting/insertion more difficult or could impede it. Similarly, it is possible that even if membrane insertion takes place, the absence of this phosphorylated sites could reduce the time of residence of these receptors at the plasma membrane by increasing its internalization and/or reducing its recycling back to this organelle. All these possibilities, together with the intrinsic activity of α_{1D}-ARs, might explain why with

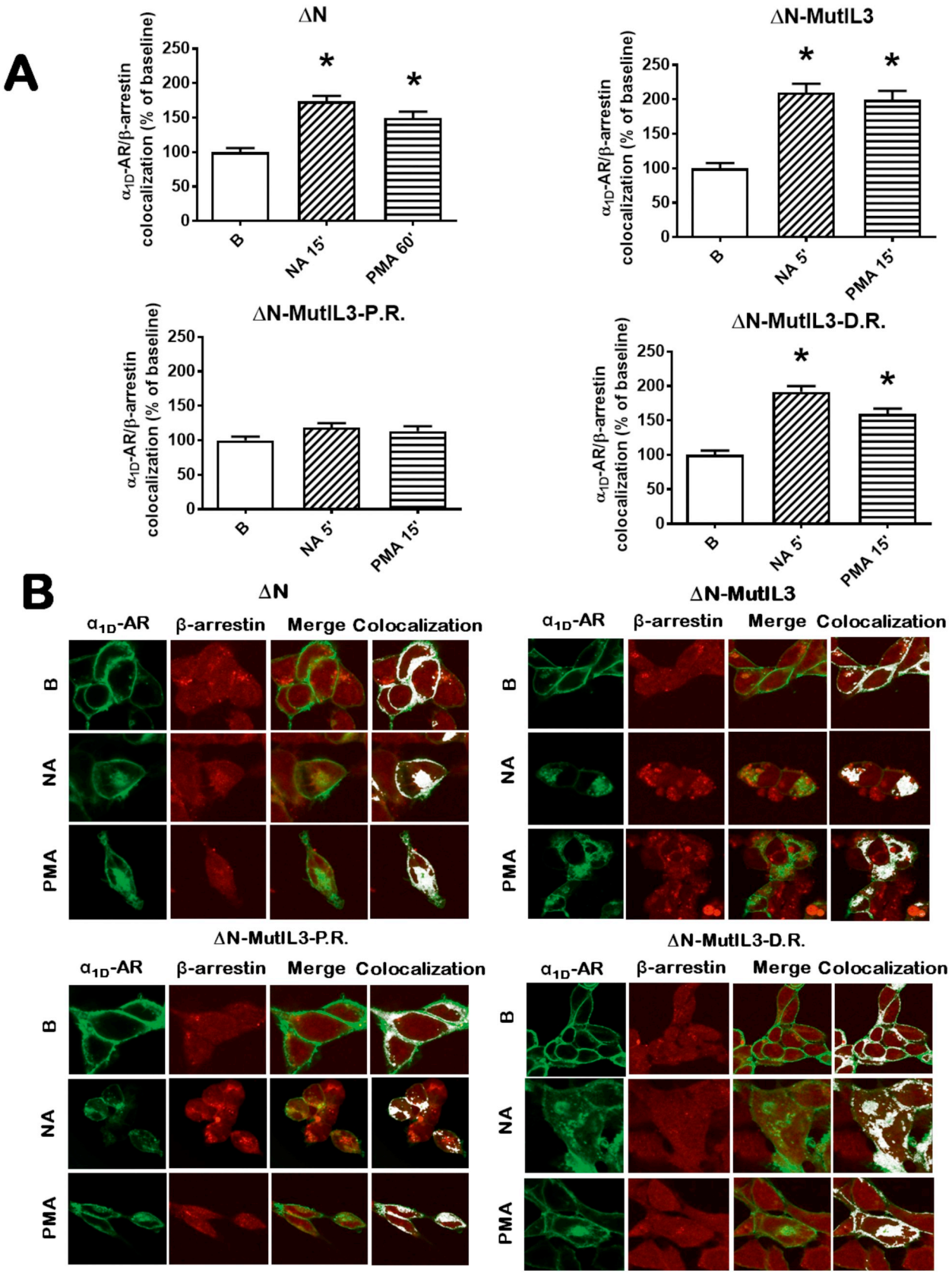

Fig. 11. Colocalization of the α_{1D}-AR mutants with endogenous β-arrestin 1/2. Panel A. Cells expressing the ΔN, ΔN-MutIL3, ΔN-MutIL3-P.R., and ΔN-MutIL3-D.R. mutants were treated without any agent (B, baseline) or stimulated with NA 10 μM or PMA 1 μM for the times at which each mutant showed a higher level of internalization (i. e., 5,. 15 or 30 min, as indicated in each histogram). Data were normalized considering the baseline colocalization observed, under baseline conditions, as 100%. Plotted are the means and vertical lines representing S.E.M. of 7 independent experiments in each of which 3–5 cells were analyzed (n = 20–35). * $P < 0.05$ vs. baseline (B). Panel B. Representative images are presented showing the α_{1D}-AR mutants (α_{1D}-AR, green channel), β-arrestins 1/2 (β-arrestins, red channel), merge images (merge) and colocalization (colocalization, white); treated as indicated; B, baseline, NA 10 μM or PMA 1 μM.

this receptor subtype, a relatively high degree of baseline phosphorylation was consistently observed [22–24,26,27]. In fact, S516 and S518 were detected as phosphorylated under baseline conditions in our work using mass spectrometry [22]. It is possible, therefore, to suggest that during receptor internalization and recycling processes, a series of different protein kinases and phosphatases could participate, forming functional elements of the signaling complexes, in a dynamic fashion.

Modification of the proximal cluster (T477, S486, and S492) with non-phosphorylatable amino acids also induces an important intracellular localization of these receptors, but substitution with aspartate did not favor their presence at the plasma membrane. This suggests that the proximal cluster might also play a role in receptor subcellular distribution but one of minor importance.

Interestingly, the ΔN-ΔC and ΔN-MutIL3-ΔC mutants exhibited a very high degree of internal localization as compared with the remainder of the mutants. This suggests the possibility that the CTail might exert a pivotal influence on the subcellular localization of this receptor. It is possible that, in addition to the detected phosphorylation sites, other undetected phosphorylation sites and/or structural elements in the CTail could have an impact on the expression of this GPCR at the plasma membrane.

The functional data obtained in this work are also worth considering. Previous information had shown that CTail truncation (i.e., the ΔNΔC mutants) did not decrease the ability of NA to increase intracellular calcium concentration [22,24], the latter being a G protein-triggered action. However, substitution of the phosphorylation sites with non-phosphorylatable amino acids leads the ΔN-MutIL3 receptor mutant to exhibit a partially decreased ability to increase intracellular calcium in response to NA; similar data were obtained for the ΔNΔC-MutIL3, as previously reported [22]. In addition, it was observed in this work that all of the different mutants of the CTail containing non-phosphorylatable amino acid substitutions exhibited a decreased calcium response to NA. In contrast, mutants with aspartate substitution in the clusters maintain the ability to increase intracellular calcium in response to the adrenergic agonist, either partially (ΔN-MutIL3-P. C. Asp mutant) or completely (ΔN-MutIL3-D. C. Asp and ΔN-MutIL3-T. M. Asp mutants). With these mutants there seems to exist a correlation between their ability to increase intracellular calcium in response to NA and their localization at the plasma membrane. In the case for the ΔNΔC mutant, there was a large accumulation of receptors in intracellular vesicles but nonetheless, a full calcium response was observed [22,24]; with the ΔNΔC-MutIL3 mutant NA-induced calcium response was smaller (confirmed in the present work, data not shown). It is likely, therefore, that membrane localization and an unmodified IL3 are critical for proper α_{1D}-AR-Gq interaction and consequent calcium signaling; however, we cannot discard the possibility that phosphorylatable residues or structural elements in the α_{1D}-AR CTail might participate in the interaction with Gq.

The ability of the different α_{1D}-AR receptor mutants to increase ERK 1/2 phosphorylation was studied. This is a signaling process that governs cell proliferation, differentiation and survival and it is modulated through many cellular pathways [32,59]. Not surprisingly, it was observed that both the expression of β-arrestin 1/2, and EGF receptor transactivation play roles in this action. We evaluated NA-activated ERK 1/2 phosphorylation in cells expressing the different receptors, and our results indicated that the kinetic profile of activation was very similar for all receptors containing the MutIL3 non-phosphorylatable mutation (i. e., a rapid and essentially sustained activation for up to 60 min) but different from what was observed with the ΔN receptor (i. e., a rapid activation that progressively decreased after 30 min); this is consistent with previous observations [22] and suggests the possibility that phosphorylation of IL3 plays a major role in turning off ERK 1/2 activation. Receptors containing the ΔN-MutIL3 mutation and non-phosphorylatable substitutions in the CTail markedly activated the ERK 1/2 pathway, but were defective in increasing intracellular calcium in response to NA, i.e., they behaved as biased receptors.

It has been observed that phosphorylation of a given GPCR can take place at different sites, depending on cell type and other conditions, and that this is associated with different functional outcomes. The possibility that such an association could be causally related has been suggested and has been denominated the bar-code hypothesis [60–62]. Efforts to characterize phosphorylation sites of different GPCRs and their functional significance have been reported (see, for example, [22,39,63–69]). The data presented here, supports the phosphorylation bar-code concept and indicates a new role for GPCR phosphorylation (i. e., one favoring membrane localization). If this is unique feature of α_{1D}-ARs or can be generalized for other GPCRs remains to be determined.

5. Conclusions

Our present results suggests that phosphorylation of a CTail distal cluster (T507, S515, S516 and S518) favors α_{1D}-AR localization at the plasma membrane, i. e., substitution of these residues for non-phosphorylatable amino acids results in the intracellular accumulation of the receptors, whereas phospho-mimetic substitution allows plasma membrane localization. Substitution of IL3 phosphorylation sites for non-phosphorylatable amino acids resulted in agonist-induced sustained ERK1/2 activation, which was not altered by additional mutations in the phosphorylated residues in the CTail. In contrast, mobilization of intracellular calcium appears to be controlled by IL3 and CTail phosphorylation states. IL3 mutation affects, differentially, NA- and PMA-induced receptor internalization and substitution of the CTail phosphorylation sites seems also to participate in this process.

Funding

This research was supported by Grants from Consejo Nacional de Ciencia y Tecnología(CONACYT) [Grant numbers 253156 and Fronteras 882] https://www.conacyt.gob.mx/ and Dirección General de Personal Académico-UNAM [PAPIIT, Grant number IN200915] http://dgapa.unam.mx/.

Declarations of interest

None.

Acknowledgments

The authors express their gratitude for advice and technical support to Dr. Maria Teresa Romero-Ávila from our laboratory and the following members of the indicated service units of our Institute: Dr. Héctor Malagón and Dr. Claudia Rivera (Bioterio); Dr. Fernando García, Dr. Ruth Rincón-Heredia, and Abrahan Rosas-Arellano (Microscopía); Juan Barbosa and Gerardo Coello (Cómputo); Dr. María Luisa Durán-Pastén (Canalopatías); and Aurey Hernández and Manuel Ortín (Taller) for their advice and technical support. Gabriel Carmona-Rosas is a doctoral student from Programa de Doctorado en Ciencias Biomédicas, Universidad Nacional Autónoma de México, and received a doctoral fellowship (CVU: 695329) from Consejo Nacional de Ciencia y Tecnología (CONACyT).

Appendix A. Supplementary data

Supplementary data to this article can be found online at https://doi.org/10.1016/j.cellsig.2018.11.003.

References

[1] R. Fredriksson, H.B. Schioth, The repertoire of G-protein-coupled receptors in fully sequenced genomes, Mol. Pharmacol. 67 (5) (2005) 1414–1425.
[2] J.P. Overington, B. Al-Lazikani, A.L. Hopkins, How many drug targets are there? Nat. Rev. Drug Discov. 5 (12) (2006) 993–996.
[3] K. Sriram, P.A. Insel, G Protein-coupled Receptors as Targets for Approved drugs:

how many Targets and how many drugs? Mol. Pharmacol. 93 (4) (2018) 251–258.
[4] J.P, D.B. Bylund Hieble, D.E. Clarke, D.C. Eikenburg, S.Z. Langer, R.J. Lefkowitz, K.P. Minneman, R.R. Ruffolo, International Union of Pharmacology. X. Recommendation for nomenclature of alpha 1-adrenoceptors: consensus update, Pharmacol. Rev. 47 (2) (1995) 267–270.
[5] M. Yang, F. Verfurth, R. Buscher, M.C. Michel, Is alpha1D-adrenoceptor protein detectable in rat tissues? Naunyn Schmiedeberg's Arch. Pharmacol. 355 (4) (1997) 438–446.
[6] D.F. McCune, S.E. Edelmann, J.R. Olges, G.R. Post, B.A. Waldrop, D.J. Waugh, D.M. Perez, M.T. Piascik, Regulation of the cellular localization and signaling properties of the alpha(1B)- and alpha(1D)-adrenoceptors by agonists and inverse agonists, Mol. Pharmacol. 57 (4) (2000) 659–666.
[7] C. Hague, Z. Chen, A.S. Pupo, N.A. Schulte, M.L. Toews, K.P. Minneman, The N terminus of the human {alpha}1D-adrenergic receptor prevents cell surface expression, J. Pharmacol. Exp. Ther. 309 (1) (2004) 388–397.
[8] A.S. Pupo, M.A. Uberti, K.P. Minneman, N-terminal truncation of human alpha1D-adrenoceptors increases expression of binding sites but not protein, Eur. J. Pharmacol. 462 (1–3) (2003) 1–8.
[9] D. Chalothorn, D.F. McCune, S.E. Edelmann, M.L. García-Cazarin, G. Tsujimoto, M.T. Piascik, Differences in the cellular localization and agonist-mediated internalization properties of the alpha(1)-adrenoceptor subtypes, Mol. Pharmacol. 61 (5) (2002) 1008–1016.
[10] J.A. García-Sáinz, M.E. Torres-Padilla, Modulation of basal intracellular calcium by inverse agonists and phorbol myristate acetate in rat-1 fibroblasts stably expressing alpha1d-adrenoceptors, FEBS Lett. 443 (3) (1999) 277–281.
[11] J.A. García-Sáinz, M.T. Romero-Ávila, L.C. Medina, Alpha(1D)-Adrenergic receptors constitutive activity and reduced expression at the plasma membrane, Methods Enzymol. 484 (2010) 109–125.
[12] R. Gisbert, M.A. Noguera, M.D. Ivorra, P. D'Ocon, Functional evidence of a constitutively active population of alpha(1D)-adrenoceptors in rat aorta, J. Pharmacol. Exp. Ther. 295 (2) (2000) 810–817.
[13] R. Gisbert, K. Ziani, R. Miquel, M.A. Noguera, M.D. Ivorra, E. Anselmi, P. D'Ocon, Pathological role of a constitutively active population of alpha(1D)-adrenoceptors in arteries of spontaneously hypertensive rats, Br. J. Pharmacol. 135 (1) (2002) 206–216.
[14] M.A. Noguera, M.D. Ivorra, P. D'Ocon, Functional evidence of inverse agonism in vascular smooth muscle, Br. J. Pharmacol. 119 (1) (1996) 158–164.
[15] Z. Chen, C. Hague, R.A. Hall, K.P. Minneman, Syntrophins regulate alpha1D-adrenergic receptors through a PDZ domain-mediated interaction, J. Biol. Chem. 281 (18) (2006) 12414–12420.
[16] I.A. Gallardo-Ortiz, S.N. Rodriguez-Hernandez, J.J. Lopez-Guerrero, L. Del Valle-Mondragon, P. Lopez-Sanchez, R.M. Touyz, R. Villalobos-Molina, Role of alpha1D -adrenoceptors in vascular wall hypertrophy during angiotensin II-induced hypertension, Auton. Autacoid Pharmacol. 35 (3) (2015) 17–31.
[17] J.S. Lyssand, M.C. Defino, X.B. Tang, A.L. Hertz, D.B. Feller, J.L. Wacker, M.E. Adams, C. Hague, Blood pressure is regulated by an {alpha}1D-adrenergic receptor/dystrophin signalosome, J. Biol. Chem. 283 (27) (2008) 18792–18800.
[18] A. Tanoue, Y. Nasa, T. Koshimizu, H. Shinoura, S. Oshikawa, T. Kawai, S. Sunada, S. Takeo, G. Tsujimoto, The alpha(1D)-adrenergic receptor directly regulates arterial blood pressure via vasoconstriction, J. Clin. Invest. 109 (6) (2002) 765–775.
[19] R. Villalobos-Molina, M. Ibarra, Alpha 1-adrenoceptors mediating contraction in arteries of normotensive and spontaneously hypertensive rats are of the alpha 1D or alpha 1A subtypes, Eur. Aust. J. Pharm. 298 (3) (1996) 257–263.
[20] R. Villalobos-Molina, M. Ibarra, Increased expression and function of vascular alpha1D-adrenoceptors may mediate the prohypertensive effects of angiotensin II, Mol. Interv. 5 (6) (2005) 340–342.
[21] C. Hague, M.A. Uberti, Z. Chen, R.A. Hall, K.P. Minneman, Cell surface expression of {alpha}1D-adrenergic receptors is controlled by heterodimerization with {alpha} 1B-adrenergic receptors, J. Biol. Chem. 279 (15) (2004) 15541–15549.
[22] M.A. Alfonzo-Méndez, G. Carmona-Rosas, D.A. Hernández-Espinosa, M.T. Romero-Ávila, J.A. García-Sáinz, Different phosphorylation patterns regulate alpha1D-adrenoceptor signaling and desensitization, Biochim. Biophys. Acta 1865 (6) (2018) 842–854.
[23] M.A. Alfonzo-Méndez, J.A. Castillo-Badillo, M.T. Romero-Ávila, R. Rivera, J. Chun, J.A. García-Sáinz, Carboxyl terminus-truncated alpha1D-adrenoceptors inhibit the ERK pathway, Naunyn Schmiedeberg's Arch. Pharmacol. 389 (8) (2016) 911–920.
[24] C.E. Rodríguez-Pérez, M.T. Romero-Ávila, G. Reyes-Cruz, J.A. García-Sáinz, Signaling properties of human alpha(1D)-adrenoceptors lacking the carboxyl terminus: intrinsic activity, agonist-mediated activation, and desensitization, Naunyn Schmiedeberg's Arch. Pharmacol. 380 (2) (2009) 99–107.
[25] T.S. Kountz, K.S. Lee, S. Aggarwal-Howarth, E. Curran, J.M. Park, D.A. Harris, A. Stewart, J. Hendrickson, N.D. Camp, A. Wolf-Yadlin, E.H. Wang, J.D. Scott, C. Hague, Endogenous N-terminal domain cleavage modulates alpha1D-adrenergic receptor pharmacodynamics, J. Biol. Chem. 291 (35) (2016) 18210–18221.
[26] J.A. García-Sáinz, C.E. Rodríguez-Pérez, M.T. Romero-Ávila, Human alpha-1D adrenoceptor phosphorylation and desensitization, Biochem. Pharmacol. 67 (2004) 1853–1858.
[27] J.A. García-Sáinz, F.G. Vázquez-Cuevas, M.T. Romero-Ávila, Phosphorylation and desensitization of alpha1d-adrenergic receptors, Biochem. J. 353 (2001) 603–610 Pt 3.
[28] K. Eichel, M. von Zastrow, Subcellular organization of GPCR signaling, Trends Pharmacol. Sci. 39 (2) (2018) 200–208.
[29] S.K. Shenoy, R.J. Lefkowitz, Beta-Arrestin-mediated receptor trafficking and signal transduction, Trends Pharmacol. Sci. 32 (9) (2011) 521–533.
[30] R.J. Lefkowitz, A brief history of G-protein coupled receptors (Nobel Lecture), Angew Chem. Int. Ed. Engl. 52 (25) (2013) 6366–6378.
[31] A.R. Thomsen, B. Plouffe, T.J. Cahill 3rd, A.K. Shukla, J.T. Tarrasch, A.M. Dosey, A.W. Kahsai, R.T. Strachan, B. Pani, J.P. Mahoney, L. Huang, B. Breton, F.M. Heydenreich, R.K. Sunahara, G. Skiniotis, M. Bouvier, R.J. Lefkowitz, GPCR-G protein-beta-arrestin super-complex mediates sustained G protein signaling, Cell 166 (4) (2016) 907–919.
[32] G. Carmona-Rosas, R. Alcantara-Hernandez, D.A. Hernandez-Espinosa, Dissecting the signaling features of the multi-protein complex GPCR/beta-arrestin/ERK1/2, Eur. J. Cell Biol. 97 (5) (2018) 349–358.
[33] C.A. Moore, S.K. Milano, J.L. Benovic, Regulation of receptor trafficking by GRKs and arrestins, Annu. Rev. Physiol. 69 (2007) 451–482.
[34] S.E. Avendaño-Vázquez, A. García-Caballero, J.A. García-Sáinz, Phosphorylation and desensitization of the lysophosphatidic acid receptor LPA1, Biochem. J. 385 (2005) 677–684 Pt 3.
[35] J.A. Castillo-Badillo, O.B. Sánchez-Reyes, M.A. Alfonzo-Méndez, M.T. Romero-Ávila, G. Reyes-Cruz, J.A. García-Sáinz, alpha1B-adrenergic receptors differentially associate with rab proteins during homologous and heterologous desensitization, PLoS One 10 (3) (2015) e0121165.
[36] R.J. Ward, E. Alvarez-Curto, G. Milligan, Using the Flp-in T-Rex system to regulate GPCR expression, Methods Mol. Biol. 746 (2011) 21–37.
[37] G. Grynkiewicz, M. Poenie, R.Y. Tsien, A new generation of Ca2+ indicators with greatly improved fluorescence properties, J. Biol. Chem. 260 (6) (1985) 3440–3450.
[38] U.K. Laemmli, Cleavage of structural proteins during the assembly of the head of bacteriophage T4, Nature 227 (5259) (1970) 680–685.
[39] R. Alcántara-Hernández, A. Hernández-Méndez, M.T. Romero-Ávila, M.A. Alfonzo-Méndez, A.S. Pupo, J.A. García-Sáinz, Noradrenaline, oxymetazoline and phorbol myristate acetate induce distinct functional actions and phosphorylation patterns of alpha1A-adrenergic receptors, Biochim. Biophys. Acta 1864 (12) (2017) 2378–2388.
[40] T.J. Collins, ImageJ for microscopy, BioTechniques 43 (1 Suppl) (2007) 25–30.
[41] M. Hachet-Haas, N. Converset, O. Marchal, H. Matthes, S. Gioria, J.L. Galzi, S. Lecat, FRET and colocalization analyzer–a method to validate measurements of sensitized emission FRET acquired by confocal microscopy and available as an ImageJ Plug-in, Microsc. Res. Tech. 69 (12) (2006) 941–956.
[42] S.M. Hartig, Basic image analysis and manipulation in ImageJ, Curr. Protoc. Mol. Biol 14 (2013) 15.1–15.12.
[43] B. Chazotte, Labeling membrane glycoproteins or glycolipids with fluorescent wheat germ agglutinin, Cold Spring Harb. Protoc. (5) (2011).
[44] L. Chen, R.R. Hodges, C. Funaki, D. Zoukhri, R.J. Gaivin, D.M. Perez, D.A. Dartt, Effects of alpha1D-adrenergic receptors on shedding of biologically active EGF in freshly isolated lacrimal gland epithelial cells, Am. J. Physiol. Cell Physiol. 291 (5) (2006) C946–C956.
[45] A. Levitzki, E. Mishani, Tyrphostins and other tyrosine kinase inhibitors, Annu. Rev. Biochem. 75 (2006) 93–109.
[46] D.S. Kang, X. Tian, J.L. Benovic, Role of beta-arrestins and arrestin domain-containing proteins in G protein-coupled receptor trafficking, Curr. Opin. Cell Biol. 27 (2014) 63–71.
[47] S.K. Shenoy, R.J. Lefkowitz, Seven-transmembrane receptor signaling through beta-arrestin, Science (308) (2005) cm10.
[48] J.A. García-Sáinz, J. Vázquez-Prado, L.C. Medina, Alpha 1-adrenoceptors: function and phosphorylation, Eur. J. Pharmacol. 389 (1) (2000) 1–12.
[49] J.A. García-Sáinz, R. Villalobos-Molina, The elusive alpha(1D)-adrenoceptor: molecular and cellular characteristics and integrative roles, Eur. J. Pharmacol. 500 (1–3) (2004) 113–120.
[50] R. Villalobos-Molina, M. Ibarra, Vascular alpha 1D-adrenoceptors: are they related to hypertension? Arch. Med. Res. 30 (5) (1999) 347–352.
[51] R. Villalobos-Molina, J.J. López-Guerrero, M. Ibarra, Functional evidence of alpha1D-adrenoceptors in the vasculature of young and adult spontaneously hypertensive rats, Br. J. Pharmacol. 126 (7) (1999) 1534–1536.
[52] S.A. Beausoleil, J. Villen, S.A. Gerber, J. Rush, S.P. Gygi, A probability-based approach for high-throughput protein phosphorylation analysis and site localization, Nat. Biotechnol. 24 (10) (2006) 1285–1292.
[53] A.K. Shukla, A. Manglik, A.C. Kruse, K. Xiao, R.I. Reis, W.C. Tseng, D.P. Staus, D. Hilger, S. Uysal, L.Y. Huang, M. Paduch, P. Tripathi-Shukla, A. Koide, S. Koide, W.I. Weis, A.A. Kossiakoff, B.K. Kobilka, R.J. Lefkowitz, Structure of active beta-arrestin-1 bound to a G-protein-coupled receptor phosphopeptide, Nature 497 (7447) (2013) 137–141.
[54] S.C. Sensken, M.H. Graler, Down-regulation of S1P1 receptor surface expression by protein kinase C inhibition, J. Biol. Chem. 285 (9) (2010) 6298–6307.
[55] A.M. Abramian, E. Comenencia-Ortiz, A. Modgil, T.N. Vien, Y. Nakamura, Y.E. Moore, J.L. Maguire, M. Terunuma, P.A. Davies, S.J. Moss, Neurosteroids promote phosphorylation and membrane insertion of extrasynaptic GABAA receptors, Proc. Natl. Acad. Sci. U. S. A. 111 (19) (2014) 7132–7137.
[56] E. Comenencia-Ortiz, S.J. Moss, P.A. Davies, Phosphorylation of GABAA receptors influences receptor trafficking and neurosteroid actions, Psychopharmacology 231 (17) (2014) 3453–3465.
[57] C. Kibaly, A.Y. Kam, H.H. Loh, P.Y. Law, Naltrexone facilitates learning and delays extinction by increasing AMPA receptor phosphorylation and membrane insertion, Biol. Psychiatry 79 (11) (2016) 906–916.
[58] D.T. Lin, Y. Makino, K. Sharma, T. Hayashi, R. Neve, K. Takamiya, R.L. Huganir, Regulation of AMPA receptor extrasynaptic insertion by 4.1N, phosphorylation and palmitoylation, Nat. Neurosci. 12 (7) (2009) 879–887.
[59] W. Kolch, Meaningful relationships: the regulation of the Ras/Raf/MEK/ERK pathway by protein interactions, Biochem. J. 351 (Pt 2) (2000) 289–305.
[60] A.B. Tobin, G-protein-coupled receptor phosphorylation: where, when and by whom, Br. J. Pharmacol. 153 (Suppl. 1) (2008) S167–S176.
[61] A.B. Tobin, A.J. Butcher, K.C. Kong, Location, location, location...Site-specific GPCR phosphorylation offers a mechanism for cell-type-specific signalling, Trends Pharmacol. Sci. 29 (8) (2008) 413–420.
[62] I. Torrecilla, E.J. Spragg, B. Poulin, P.J. McWilliams, S.C. Mistry, A. Blaukat, A.B. Tobin, Phosphorylation and regulation of a G protein-coupled receptor by protein kinase CK2, J. Cell Biol. 177 (1) (2007) 127–137.
[63] M. Bouzo-Lorenzo, I. Santo-Zas, M. Lodeiro, R. Nogueiras, F.F. Casanueva, M. Castro, Y. Pazos, A.B. Tobin, A.J. Butcher, J.P. Camina, Distinct phosphorylation

sites on the ghrelin receptor, GHSR1a, establish a code that determines the functions of ss-arrestins, Sci. Rep. 6 (2016) 22495.
[64] A.J. Butcher, B.D. Hudson, B. Shimpukade, E. Alvarez-Curto, R. Prihandoko, T. Ulven, G. Milligan, A.B. Tobin, Concomitant action of structural elements and receptor phosphorylation determine arrestin-3 interaction with the free fatty acid receptor FFA4, J. Biol. Chem. 289 (26) (2014) 18451–18465.
[65] A.J. Butcher, R. Prihandoko, K.C. Kong, P. McWilliams, J.M. Edwards, A. Bottrill, S. Mistry, A.B. Tobin, Differential G-protein-coupled receptor phosphorylation provides evidence for a signaling bar code, J. Biol. Chem. 286 (13) (2011) 11506–11518.
[66] R. Prihandoko, E. Alvarez-Curto, B.D. Hudson, A.J. Butcher, T. Ulven, A.M. Miller, A.B. Tobin, G. Milligan, Distinct phosphorylation clusters determine the signaling outcome of free fatty acid receptor 4/G protein-coupled receptor 120, Mol. Pharmacol. 89 (5) (2016) 505–520.
[67] D. Zindel, S. Engel, A.R. Bottrill, J.P. Pin, L. Prezeau, A.B. Tobin, M. Bunemann, C. Krasel, A.J. Butcher, Identification of key phosphorylation sites in PTH1R that determine arrestin3 binding and fine-tune receptor signaling, Biochem. J. 473 (22) (2016) 4173–4192.
[68] X. Chen, B. Bai, Y. Tian, H. Du, J. Chen, Identification of serine 348 on the apelin receptor as a novel regulatory phosphorylation site in apelin-13-induced G protein-independent biased signaling, J. Biol. Chem. 289 (45) (2014) 31173–31187.
[69] L. Bray, C. Froment, P. Pardo, C. Candotto, O. Burlet-Schiltz, J.M. Zajac, C. Mollereau, L. Mouledous, Identification and functional characterization of the phosphorylation sites of the neuropeptide FF2 receptor, J. Biol. Chem. 289 (49) (2014) 33754–33766.